

Epidemiological impact and cost-effectiveness analysis of COVID-19 vaccination in Kenya

Stacey Orangi ^{1,2}, John Ojal,^{3,4} Samuel PC Brand,^{5,6} Cameline Orlando,³ Angela Kairu ¹, Rabia Aziza,^{5,6} Morris Ogero,³ Ambrose Agweyu ^{3,7}, George M Warimwe,^{3,7} Sophie Uyoga,³ Edward Otieno,³ Lynette I Ochola-Oyier,³ Charles N Agoti,³ Kadondi Kasera,⁸ Patrick Amoth,⁸ Mercy Mwangangi,⁸ Rashid Aman,⁸ Wangari Ng'ang'a,⁹ Ifedayo MO Adetifa,^{3,4} J Anthony G Scott,^{3,4} Philip Bejon,^{3,7} Matt J Keeling,^{5,6,10} Stefan Flasche,⁴ D James Nokes,^{3,5,6} Edwine Barasa ^{1,2,7}

To cite: Orangi S, Ojal J, Brand SPC, *et al*. Epidemiological impact and cost-effectiveness analysis of COVID-19 vaccination in Kenya. *BMJ Global Health* 2022;**7**:e009430. doi:10.1136/bmjgh-2022-009430

Handling editor Lei Si

► Additional supplemental material is published online only. To view, please visit the journal online (<http://dx.doi.org/10.1136/bmjgh-2022-009430>).

DJN and EB contributed equally. SO and JO contributed equally.

Received 22 April 2022
Accepted 22 June 2022



© Author(s) (or their employer(s)) 2022. Re-use permitted under CC BY-NC. No commercial re-use. See rights and permissions. Published by BMJ.

For numbered affiliations see end of article.

Correspondence to

Stacey Orangi;
sorangi@kemri-wellcome.org and
Dr John Ojal;
jonal@kemri-wellcome.org

ABSTRACT

Background A few studies have assessed the epidemiological impact and the cost-effectiveness of COVID-19 vaccines in settings where most of the population had been exposed to SARS-CoV-2 infection.

Methods We conducted a cost-effectiveness analysis of COVID-19 vaccine in Kenya from a societal perspective over a 1.5-year time frame. An age-structured transmission model assumed at least 80% of the population to have prior natural immunity when an immune escape variant was introduced. We examine the effect of slow (18 months) or rapid (6 months) vaccine roll-out with vaccine coverage of 30%, 50% or 70% of the adult (>18 years) population prioritising roll-out in those over 50-years (80% uptake in all scenarios). Cost data were obtained from primary analyses. We assumed vaccine procurement at US\$7 per dose and vaccine delivery costs of US\$3.90–US\$6.11 per dose. The cost-effectiveness threshold was US\$919.11.

Findings Slow roll-out at 30% coverage largely targets those over 50 years and resulted in 54% fewer deaths (8132 (7914–8373)) than no vaccination and was cost saving (incremental cost-effectiveness ratio, ICER=US\$–1343 (US\$–1345 to US\$–1341) per disability-adjusted life-year, DALY averted). Increasing coverage to 50% and 70%, further reduced deaths by 12% (810 (757–872) and 5% (282 (251–317) but was not cost-effective, using Kenya's cost-effectiveness threshold (US\$919.11). Rapid roll-out with 30% coverage averted 63% more deaths and was more cost-saving (ICER=US\$–1607 (US\$–1609 to US\$–1604) per DALY averted) compared with slow roll-out at the same coverage level, but 50% and 70% coverage scenarios were not cost-effective.

Interpretation With prior exposure partially protecting much of the Kenyan population, vaccination of young adults may no longer be cost-effective.

INTRODUCTION

As of late May 2022, Kenya has experienced five distinct waves of the COVID-19 pandemic

WHAT IS ALREADY KNOWN ON THIS TOPIC

- ⇒ The COVID-19 pandemic has led to a substantial number of cases and deaths globally and COVID-19 vaccines are considered the main strategy of curtailing the pandemic. However, many African nations are still at the early phase of vaccination.
- ⇒ Evidence on the cost-effectiveness of COVID-19 vaccines is useful in estimating value for money and illustrate opportunity costs. Though, there is a need to balance these economic outcomes against the potential impact of vaccination.

WHAT THIS STUDY ADDS

- ⇒ In Kenya, a targeted vaccination strategy that prioritises those of an older age and is deployed at a rapid roll-out speed achieves greater marginal health impacts and is better value for money.
- ⇒ Given the existing high-level population protection to COVID-19 due to prior exposure, vaccination of younger adults is less cost-effective in Kenya.

HOW THIS STUDY MIGHT AFFECT RESEARCH, PRACTICE OR POLICY

- ⇒ Rapid deployment of vaccines during a pandemic averts more cases, hospitalisations and deaths and is more cost-effective.
- ⇒ Against a context of constrained fiscal space for health, it is likely more prudent for Kenya to target those at severe risk of disease and possibly other vulnerable populations rather than to the whole population.

with more than 320 000 reported cases and 5600 deaths.¹ While at the global level vaccines to prevent severe disease from SARS-CoV-2 are the main strategy for curtailing the pandemic burden on health,² most African nations are still at a very early phase of vaccine roll-out, particularly in tropical sub-Saharan Africa,

with most countries at less than 10% of the adult population fully vaccinated.¹ However, in contrast to other part of the world where low vaccine coverage in high-risk groups has led to high mortality even from the omicron variant,³ in Kenya cross-sectional serological surveys of anti-SARS-CoV-2 spike protein antibodies together with transmission dynamic model forecasts indicate that about 80% of the population have been exposed to the virus at least once and thus generated considerable immunity⁴ with similar estimates in the region.⁵ This raises the question what additional benefit can vaccination still have in mitigating future disease burden from COVID-19?

The Kenyan government is pursuing a phased COVID-19 vaccination strategy that aims to follow a risk-prioritisation matrix leading sequentially to the vaccination of all adults by December 2022.⁶ The prioritised population are an estimated 30% of the adult population and include health and other essential workers, individuals at high risk of severe disease (those above 58 years, and those above 18 years with comorbidities), and individuals at high risk of infection (individuals in congregate settings, and those working in hospitality and transport sectors).⁶ Vaccine roll-out commenced in early March 2021. As of late May, 2022 more than 18.1 million doses had been administered with 31% of Kenya's adult population above the age of 18 years being fully vaccinated.⁷ The initial procurement comprised of the Oxford/Astra Zeneca vaccine mainly sourced through the COVID-19 Vaccines Global Access Facility (COVAX) mechanism and bilateral negotiations, evolving more recently to a multivaccine type deployment through additional sources including the African Union's African Vaccine Acquisition Task Team mechanism.⁶

Economic evaluations are useful in providing evidence of the value for money for different health interventions and illustrates the opportunity costs of the interventions in a setting with many competing priorities. However, there is a need to balance these economic outcomes against the potential impact of the interventions. Therefore, this study evaluates the potential epidemiological impact and cost-effectiveness of different vaccine roll-out scenarios in a Kenyan population that has already acquired a high-level immunity due to prior infections. The study employs a partially retrospective perspective with vaccination scenarios beginning on September 2021 and with an immune escape variant striking in November 2021.

METHODS

Study setting

Kenya is a lower-middle income country with a gross domestic product (GDP) per capita of US\$1838.21.⁸ The population as of 2019 was estimated at 47.56 million with a predominantly young population: 50% of the population are 19 years and below and only 11% of the population are 50 years and above.⁹ As of late May 2022, most COVID-19 cases were reported among those aged 20–49 years (n=2 047 566, 63%), followed by those above 50 years (n=862 775, 27%), and lastly among those 0–19 years (n=333 288, 10%).¹⁰ The reported case fatality rate as of late May 2022 was 1.7% with deaths increasing with age at 3% (163 deaths) among those 0–19 years, 23% (1,292 deaths) among those 20–49 years and 74% (4194 deaths) among those above 50 years of age.¹⁰

Study design

This study is an impact and cost-effectiveness analysis of COVID-19 vaccine roll-out strategies that uses cost estimates from primary costing studies and vaccine effectiveness measures from an age structured transmission model. The costs and effects are estimated from a societal perspective for a period of 1.5 years (1 September 2021 to 28 February 2023) starting at the peak of the Kenyan delta wave and simulating the emergence of a partial immune escape variant (omicron-like) from November 2021.

Intervention comparators

Primary analysis

We carry out an incremental analysis of four vaccination coverage scenarios deployed over an 18-month period (non-rapid deployment), starting at 0% coverage in September 2021 (table 1): No vaccination (0% coverage), or 30% 50% and 70% coverage of the population older than 18 years with prioritisation of those aged 50 years and above (until 80% of those >50 years old are fully vaccinated), then the remaining doses given to those 18–49 years).

Secondary analysis

We consider a secondary analysis that assesses the same scenarios under the primary analysis but with rapid vaccine deployment in which the targeted vaccine coverage is attained within 6 months of starting vaccination.

Table 1 Intervention comparators and number vaccinated within 1.5 years' time horizon

Vaccination strategy	No of >50 years who were vaccinated (proportion of those >50 years)	No of 18-49 years who were vaccinated (proportion of those 18-49 years)
No vaccination		
30% adult coverage strategy	4 133 775 (80%)	3 186 225 (19%)
50% adult coverage strategy	4 133 775 (80%)	8 366 225 (41%)
70% adult coverage strategy	4 133 775 (80%)	13 366 225 (65%)

An assumption was made that all the vaccination coverage scenarios and deployment strategies were implemented alongside a low intensity mix of non-pharmaceutical interventions (NPIs). The low intensity NPI is matched with how government progressively lifted or modified the restrictions and refers to reopening of international borders, relaxed curfew, controlled public gatherings, controlled reopening of restaurants and bars, controlled reopening of schools, ban lift on mandatory use of masks and adherence to hand hygiene from November 2020 to the time of writing this manuscript. Further, we assume administration of the Oxford-AstraZeneca vaccine across all vaccination strategies, as it was the predominant vaccine in the country, at the time of analysis.

Transmission modelling and parameter inference

We extended a dynamic SARS-CoV-2 transmission model previously designed to estimate population level immunity from natural infection in Kenya by fitting to case notification and serological data⁴ to include additional age structure and vaccination status. In common with other approaches to modelling SARS-CoV-2 transmission,^{11 12} we assume that the rate of new infections depends on: (1) age and setting-specific contact rates within the population, (2) frequency of Alpha, Beta and Delta variants of SARS-CoV-2 among the infected subpopulation, (3) the first and second dose vaccine protection against infection in each age group which were assumed to wane over time and (4) prior primary infections. The probability of being infected with SARS-CoV-2 per infectious contact, and the chance of developing symptoms on infection, increased substantially with age (see online supplemental information and online supplemental figure 1) for details of the transmission model).

The goal of the transmission model is to project the health gains of the vaccine deployment strategies described above in comparison with the no vaccine scenario. This requires estimation of parameters pertaining to the risk of transmission, and, of risk factors associated with infection given age, and the infecting variant of SARS-CoV-2 in the Kenyan setting. These parameters were inferred by fitting the model to the following Kenyan epidemiological data (see online supplemental file 2 for inference methods).

- ▶ Daily reported numbers of positive and negative PCR tests from the Kenyan Ministry of Health COVID-19 linelist (between 1 January 2021 and 1 November 2021).
- ▶ Cross-sectional serological surveys of (1) donor samples from the Kenyan National Blood and Transfusion Service¹³ and (2) demographic surveillance systems (between 1 January 2021 and 27 May 2021).¹⁴

We used a Bayesian hierarchical inference approach aimed at allowing inference on reporting fraction in counties with higher numbers of serological tests to influence inference of reporting fraction in counties with lower numbers of serological tests (see online supplemental information) for details on underlying

data for age-specific effects and details on inference methodology).

Infection outcome modelling and risk factor inference

Bayesian inference of transmission model parameters generated a posterior predictive distribution for the number of SARS-CoV-2 infections in Kenya broken down by day, county, age of infected, infecting variant of SARS-CoV-2, and, whether it was a primary infection event or a reinfection event. We categorised the outcome of each infection as being either deadly, critical (requiring treatment in an intensive care unit (ICU)), severe (requiring in-patient hospitalisation in a general ward), mild or asymptomatic. Severe and critical infections were assumed to cause admission to a health facility's general ward or ICU for an average of 12 days postinfection. Severe infection was assumed to lead to an average 7-day stay in a general COVID-19 ward before discharge. Critical infection leads to an average 7-day stay in ICU,¹⁵ before transfer to a general COVID-19 ward for a further average 7-day stay before discharge (see online supplemental information) for details on hospital durations of stay).

Risk factors for infection outcome were inferred using reported Kenya outcome data:

- ▶ Daily reported numbers occupying general health facilities with COVID-19 as the diagnosed cause (1 March 2021–1 November 2021).
- ▶ Daily reported numbers occupying ICUs with COVID-19 as the diagnosed cause (1 March 2021–1 November 2021).
- ▶ Daily reported incidence of death with COVID-19 as the diagnosed cause (1 January 2021–1 November 2021).

Vaccination roll-out modelling

We used the fitted model to predict the course of the pandemic from 1 September 2021 (historically this was past the peak of the fourth wave of cases in Kenya) to 30 June 2023 and the impact of vaccination on, severe and critical disease, and deaths. We distribute the total number of doses planned under each vaccination scenario to the 47 counties proportionally according to population size above the age of 18 years.⁹ We assume that the number of doses given per day will be the same during the study period. Doses will be offered to adults older than 50 years first, until take up of available vaccines dropped off, which we assumed would occur once 80% of over 50s had taken up both doses. The remaining doses will subsequently be randomly allocated to all 18–50 years. Within the model, individuals are either unvaccinated, partially vaccinated (14 days after receipt of the first dose), fully vaccinated (14 days after receipt of the second dose) or have waned vaccine effectiveness. We assumed vaccine effectiveness against death (delta variant) to range from 90% to 95% after the first dose and 95% to 99% after the second dose.¹⁶ Vaccine effectiveness against severe or critical disease (delta variant) of

Table 2 Key analysis parameters

Parameter	Values (Lb; Ub)	Source
Cost-effectiveness parameters		
Treatment costs (2021 US\$)		
Per day, per patient unit cost of management of asymptomatic COVID-19	US\$19.75*testing rate	23
Per day, per patient unit cost of management of mild to moderate COVID-19	US\$19.75*testing rate	23
Per day, per patient unit cost of management of severe COVID-19	US\$129.45	23
Per day, per patient unit cost of management of critical COVID-19	US\$623.14	23
Testing rate		
†Testing rate in the population	0.52%	Proportion of reported to modelled cases
Vaccination costs (2021 US\$)		
Vaccine procurement costs per dose	US\$8.67 (Base cost: US\$7 and including importation costs)	22
Supplies procurement costs per dose	US\$0.08	22
Vaccine delivery cost per dose (no vaccination)	US\$0	22
Vaccine delivery cost per dose (30% coverage)	US\$6.11	22
Vaccine delivery cost per dose (50% coverage)	US\$4.16	22
Vaccine delivery cost per dose (70% coverage)	US\$3.90	22
Duration of disease and length of hospitalisation		
Length of hospitalisation for severe episode	7 days (4–11)	Assumption
Length of ICU stay for critical episode	7 days (4–11)	15
Duration of asymptomatic disease	7 days	Assumption
Duration of mild to moderate disease	7 days	Assumption
Duration of severe disease	12 days	27
Duration of critical disease	20 days	27
DALYs		
Disability weight for asymptomatic episode	0	
Disability weight for mild/moderate episode	0.051 (0.032; 0.074)	28
Disability weight for severe episode	0.133 (0.088; 0.191)	28
Disability weight for critical episode	0.655 (0.579; 0.727)	29
*Average age at death		9
0–19 years	9.27 years	
20–49 years	31.75 years	
50–59 years	54.10 years	
60–69 years	63.85 years	
70–79 years	73.41 years	
80+ years	86.00 years	
Life expectancy		26
0–19 years	64.10 years	
20–49 years	40.94 years	
50–59 years	24.71 years	
60–69 years	17.64 years	
70–79 years	11.41 years	
80+ years	4.84 years	
Cost-effectiveness threshold per DALY averted	US\$919.11	8 30 31
Transmission dynamic model parameters		
Transmission dynamic model values	See online supplemental table S1	
*Average age at death is based on the weighted mean age across the different age groups.		
†Testing rate: A proxy estimate is used that is calculated as a proportion of reported cases to modelled cases across all severity levels from 1 January 2021 to 19 September 2021.		
DALYs, disability-adjusted life-years; ICU, intensive care unit.		

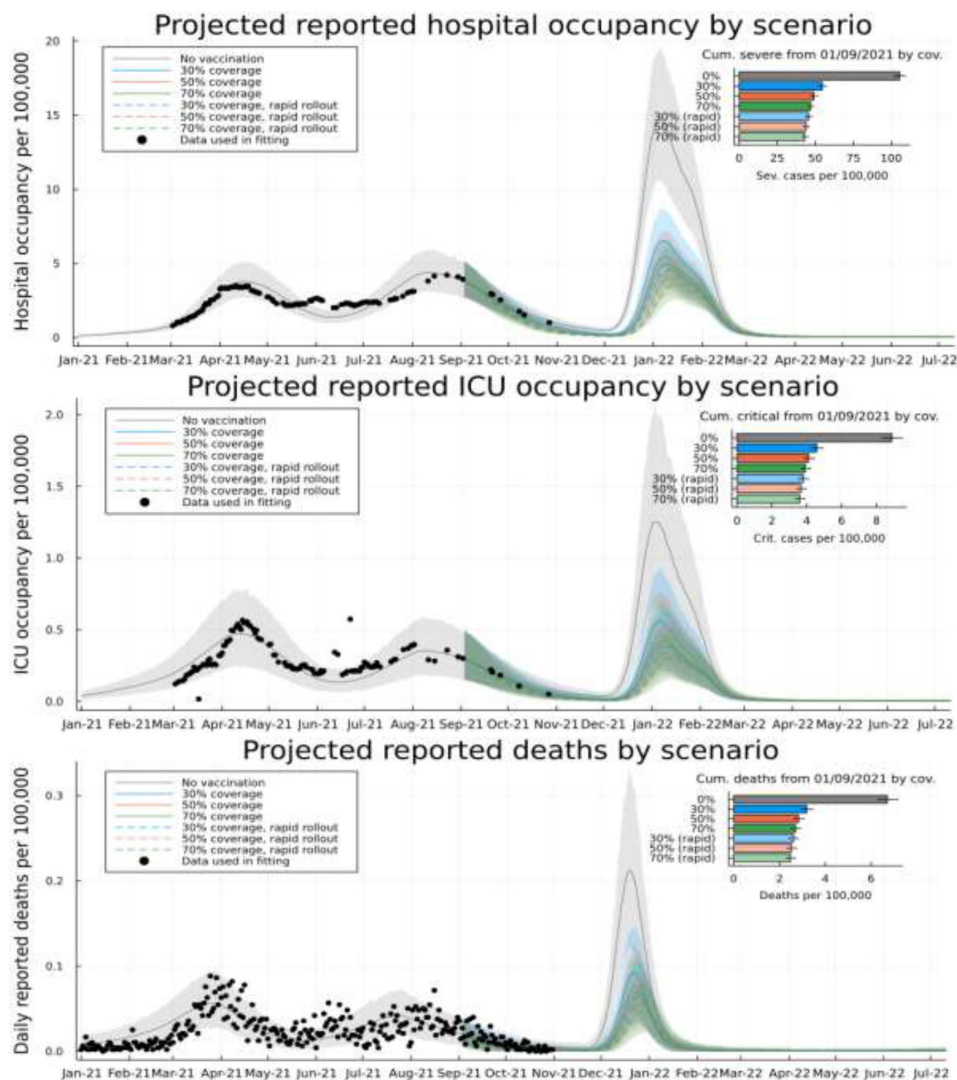


Figure 1 Model-based projections and vaccine scenarios: model-based prediction intervals for daily occupancy of general wards in health facilities in Kenya (top), daily occupancy of intensive care units in Kenya (middle) and daily reported incidence of death with COVID-19 in Kenya (bottom). All scatter points represented data used in inference of the infection outcome model. Grey curves are the posterior mean model prediction (background shading 95% CIs) with no vaccinations. Coloured curves represent a target of 30% (blue), 50% (red) and 70% (green) of over 18-year-old population in Kenya over 18 months (solid) or 6 months (dashed). Insets: projections of cumulative number of severe (top), critical (middle) and deadly (bottom) cases after 1 September 2021 under each vaccine target scenario. ICU, intensive care unit.

80%–90% and 95%–99% after the first and second dose, respectively.¹⁶ The vaccine effectiveness against acquisition of infection per infectious contact (delta variant) was 55%–65% and 65%–80% after the first and second dose, respectively.¹⁶ We assumed an effectiveness of 0%–35% and 0%–69% against onward transmission, per infection (delta variant), after either the first or second dose.¹⁷ We assume that immunity due to either past infection of vaccination eventually wanes to 70% protection against disease and 0% protection against infection, with a mean time to complete waning of 460 days after the second dose of vaccine and 5 years following natural infection.^{18 19} Furthermore, we assume that protection due to prior infection combined constructively with vaccination; that is that people who had previously had a natural infection episode of SARS-CoV-2 were further protected

from reinfection by vaccination (see online supplemental information and online supplemental figures 2–4).

Immune escape variant

The scenarios investigated in this paper involve the rapid spread of a new variant of SARS-CoV-2 that, due to evolutionary adaptation, partially avoids protection from infection due to prior naturally acquired immunity and/or vaccination. Concretely, we assume that the immune escape variant enters Kenya in early November 2021 and rapidly dominates transmission by 15 November 2021. Compared with homologous protection against reinfection with the Delta variant, the protection afforded by prior infection and/or vaccination against acquiring the novel immune escape variant is assumed to be decreased by 50%, with all epidemiological rates increased such that

Table 3 Projected clinical outcomes, costs and the cost-effectiveness of different vaccination strategies in Kenya from a societal perspective

Health outcomes		Economic outcomes				One-way sensitivity analysis of under-reporting in hospitalisations and deaths (factor of under-reporting)			
*Averted SARS-CoV-2 infections per 100 000 Median (2.5–97.5th percentile)	*Averted SARS-CoV-2 CoV-2 deaths Median (2.5–97.5th percentile)	Total costs (US\$ millions) Median (2.5–97.5th percentile)	Total DALYs (thousands) Median (2.5–97.5th percentile)	†ICER, (US\$ per DALY averted) Mean (95% CI)	ICER (4)	ICER (3)	ICER (2)	ICER (1)	
Non-rapid vaccination strategy (administered within 1.5 years)									
No vaccination	–	787 (740 to 882)	247 (243 to 252)	–	–	–	–	–	
30% coverage (24 to 38)	8132 (7914 to 8373)	614 (589 to 659)	114 (110 to 118)	–1343 (–1345 to –1341) Dominant	–905 (–907 to –902) Dominant	–175 (–178 to –173) Dominant	1278 (1275 to 1280)	5595 (5592 to 5598)	
50% coverage (3 to 5)	810 (757 to 872)	658 (636 to 699)	101 (97 to 104)	3291 (3287 to 3295) Dominant	4908 (4903 to 4913) Dominant	7598 (7592 to 7605) Dominant	12958 (12949 to 12967)	28878 (28860 to 28896)	
70% coverage (1 to 3)	282 (251 to 317)	763 (742 to 801)	96 (92 to 100)	22623 (22602 to 22645) Dominant	29075 (29048 to 29101) Dominant	39791 (39756 to 39827) Dominant	61093 (61040 to 61146)	123967 (123863 to 124072)	
Rapid vaccination strategy (administered within 6 months)									
No vaccination	–	787 (740 to 882)	247 (243 to 252)	–	–	–	–	–	
30% coverage (29 to 48)	9433 (9197 to 9711)	545 (524 to 582)	93 (89 to 96)	–1,607 (–1609 to –1604) Dominant	–1,230 (–1232 to –1227) Dominant	–603 (–605 to –600) Dominant	646 (644 to 649)	4357 (4354 to 4360)	
50% coverage (0.5 to 2)	250 (201 to 296)	620 (599 to 655)	88 (85 to 92)	18257 (18226 to 18287) Dominant	23582 (23543 to 23620) Dominant	32440 (32389 to 32491) Dominant	50096 (50020 to 50173)	102582 (102430 to 102733)	
70% coverage (–0.05 to 1)	161 (106 to 208)	731 (713 to 765)	86 (82 to 89)	44250 (44126 to 44374) Dominant	56074 (55919 to 56230) Dominant	75768 (75560 to 75976) Dominant	115100 (114788 to 115413)	232667 (232036 to 233298)	

ICER (4), ICER (3), ICER (2) and ICER (1)= under-reporting factors for hospitalisation and deaths used were 4, 3, 2 and 1, respectively. Total averted infections=rounded off to the nearest 100 000; Total Cost=rounded off to the nearest 1 000 000; Total DALY rounded off to the nearest 1000; Total deaths and ICERs=rounded off to the nearest whole number.

*Averted SARS-CoV-2 infections and deaths = This is the incremental averted infections/deaths compared with the vaccination strategy that appears in the row above.

†ICER=Baseline ICER used in analysis where under-reporting in hospitalisations and deaths is adjusted with a factor of 5.

DALYs, disability-adjusted life-years; ICER, incremental cost-effectiveness ratio.

the mean generation time of transmission is reduced by 30% compared with the transmission of the Delta variant. However, we also assume that the fundamental reproductive number and risk factors for severe, critical and deadly outcomes are unchanged compared with Delta (see online supplemental information for the details of how a 50% decrease in protection from infection was implemented).

Cost estimates

The cost estimates used in this study were derived using a hybrid method that involved both an ingredients approach (bottom-up) and a top-down approach.^{20 21} The analysis used economic costs, which reflect the opportunity cost and incorporated both recurrent and capital costs. Capital costs were annuitised using a discount rate of 3% over their useful life. Costs incurred in other years were adjusted for inflation using the GDP deflator and reported in 2021 United States Dollars. Key model cost input parameters are shown in table 2 and the three main cost components are described below. The costs of NPIs were excluded as all vaccination strategies employed the same NPI regimen (low NPI intensity) and would therefore not change the reported incremental cost-effectiveness ratios (ICERs).

Vaccination costs

We included vaccine and related supplies costs, as well as vaccine delivery costs. Vaccine and related supply costs were the economic costs to purchase the vaccine and related supplies such as syringes and safety boxes through the COVAX facility. A base cost of US\$7 was used for vaccine procurement, which is the country's procurement cost from the COVAX facility. Additionally, the freight costs, insurance costs, import declaration fees, clearance fees and the railway development levy associated with the vaccines and its supplies were included. Vaccine and syringe wastage rates of 10% were assumed.²² Vaccine delivery costs referred to costs associated with delivering COVID-19 immunisations to the adult population and were estimated across six components (1) vaccine supply chain (2) vaccine safety monitoring and adverse events following immunisation management (3) training (4) advocacy, communication and social mobilisation (5) data management, monitoring and supervision (6) vaccine administration. The resource used and costs were estimated through the analysis of programmatic budgets, and through key informant interviews. Details of the vaccine procurement and delivery cost analysis and results are reported elsewhere.²² This analysis assumed equivalent vaccine delivery costs for both the rapid and non-rapid vaccination strategies.

Treatment costs

The direct medical costs of COVID-19 treatment were sourced from a recently conducted study that examined the unit costs for COVID-19 case management in Kenya.²³ This costing analysis employed an ingredients-based

approach to estimate healthcare costs across the disease severity categories; with the exclusion of adverse events costs.²³

Productivity losses

Productivity losses due to illness and mortality were estimated using a human capital approach.²⁴ The impact of COVID-19 on lost time through illness or morbidity was estimated by accounting for the average Kenyan's productivity measure (GDP per capita) and duration of disease/duration of quarantine; the latter was used where duration of illness was less than the 14-day quarantine period in Kenya. For asymptomatic and mild disease, the testing rate was accounted for and an assumption was made that only those in the informal sector are likely not to be productive as they isolate. Further, the economic impact of COVID-19-related mortality was estimated by considering the years of life lost (YLL) because of premature mortality and the average productivity measure. We did not account for productivity losses from long COVID-19, as the burden is poorly defined in our setting (see equation (a) in the online supplemental information).

Disability-adjusted life-years

The outcome of the cost-effectiveness analysis was reported in terms of disability-adjusted life-years (DALYs); the sum of YLL and years lost due to disability²⁵ (see equations b, c and d in online supplemental information).

DALYs were calculated considering a discount rate of 3%, the Kenyan 2019 standardised life expectancies,²⁶ assumed duration of illness of 7 days for asymptomatic and mild disease and 12 and 20 days for severe and critical disease, respectively,²⁷ as well as disability weights. COVID-19 is a novel disease, and its disability weights are currently not available. Therefore, for asymptomatic COVID-19 disease we assumed a disability weight of 0. For mild-to-moderate COVID-19 symptoms and severe disease, we used disability weights from the 2013 Global Burden of disease of 0.051 (0.032–0.074) and 0.133 (0.088–0.190) assigned to infectious disease with moderate acute episodes and severe episodes, respectively.²⁸ For critical disease, we assume disability weights of 0.655 (0.579–0.727) assigned to ICU admissions.²⁹ This analysis did not incorporate age-weighting in the DALYs. These input parameters are reported in table 2.

The ICER was the measure of cost-effectiveness calculated as the net change in total costs and DALYs averted between comparators. The ICER was compared with the opportunity cost-based on Kenya's cost-effectiveness threshold (US\$919.11).^{30 31}

$$\text{ICER} = (\text{Cost}_{\text{index}} - \text{Cost}_{\text{baseline}}) / (\text{DALY}_{\text{baseline}} - \text{DALY}_{\text{index}})$$

Where

$\text{Cost}_{\text{index}}$ = cost of strategy of interest.

$\text{Cost}_{\text{baseline}}$ = cost of the next less effective strategy.

$\text{DALY}_{\text{index}}$ = total DALYs under the strategy of interest.

$\text{DALY}_{\text{baseline}}$ = total DALYs under the next less effective strategy.

ICERs are estimated within each of the two roll-out scenarios slow and rapid and are not comparable between the two vaccine-deployment cases except when the baseline is no vaccination.

Sensitivity analysis for the model

Vaccine effectiveness against different epidemiological outcomes such as the acquisition of disease, onward transmission, severe disease and death does vary with age, duration between vaccination and testing of efficacy, variant of infection and type of vaccine being used among other factors.^{32–35} Therefore, to determine the robustness of the epidemiological model predictions to the vaccine effectiveness parameter values, we performed a sensitivity analysis across a range of values using a vaccine waning effectiveness model fitted to the UK Health Security Agency COVID-19 data.^{16 17}

A univariate sensitivity analysis was done on the economic model to determine the robustness of the unit cost estimates with variations in vaccine procurement costs (base cost of US\$3 and US\$10 used) and discounting rates of DALYs (rate of 0% used). Further, given the current evidence gap to confidently determine the magnitude of underreporting of COVID-19 deaths,³⁶ the baseline cost-effectiveness analysis assumed an underreporting of hospitalisation and deaths by a factor of 5 and a one-way sensitivity analysis was done by varying the under-reporting factor (1–4).

A probabilistic sensitivity analysis to explore the influence of some economic parameters on the ICERs was done using Sobol sampling and was based on the statistical distributions in online supplemental table S2. Sobol sequences belong to the family of quasi-random sequences which are designed to generate samples of multiple parameters as uniformly as possible over the multidimensional parameter space.³⁷ For the parameters used in the probabilistic sensitivity analysis, the statistical distributions were chosen to model the available prior knowledge represented by existing data, as reported in table 2. For the cost estimates range, a 20% increase or decrease was assumed for the parameters.

All code and data for the transmission model and economic evaluation analysis underlying this study is accessible at the Github open code repository.³⁸

Patient and stakeholder involvement

No patients were involved in this study. The results of the study will be disseminated to key policy-makers and relevant stakeholders involved in COVID-19 vaccine deployment in Kenya. See online supplemental file 1 for author reflexivity.

RESULTS

Clinical impacts of vaccination strategies and scenarios

The non-rapid deployment of vaccinating 30% of the adult population results in 10% (32 (24–38) per 100 000) fewer infections, 54% (8132 (7914–8373) fewer deaths compared with no vaccination, and 978 (949–1005)

people would need to be vaccinated to prevent 1 death. An increase of vaccine coverage of the adult population to 50% results in a further 1% (4 (3–5) per 100 000) reduction in infections, a further 12% (810 (757–872) reduction in deaths, and 5617 (5218–6011) more people would need to be vaccinated to prevent an additional death. Similarly, an increase of vaccine coverage to 70% leads to a 1% reduction in cases, a 5% reduction in deaths, and 17730 (15 773–19 920) more people would need to be vaccinated to prevent an additional death compared with the 50% vaccination coverage.

In the rapid vaccine roll-out strategy, the 30% vaccine coverage averts 12% of cases preventing an average of 39 (29–48) per 100 000 infections and 63% of deaths saving an average of 9433 (9197–9711) lives compared with no vaccination. Therefore, 843 (819 to 864) people would need to be vaccinated to prevent a death. The 30% coverage under a rapid deployment averts more cases and saves more lives compared with a non-rapid roll-out with the same level of coverage (see table 3 and figure 1.)

Cost-effectiveness of vaccination strategies

Table 3 shows the total costs, DALYs and ICERs of the vaccination scenarios considered in the analysis from a societal perspective. Under the non-rapid vaccination scenario, vaccinating 30% of the adult population is cost-saving (ICER=US\$–1343 (US\$–1345 to US\$–1341) per DALY averted) and hence highly cost-effective. Increasing vaccine coverage to 50% of the adult population was not cost-effective (ICER=US\$3291 (US\$3287 to US\$3295) per DALY averted) compared with 30% coverage. Similarly, increasing vaccine coverage to 70% was deemed not cost-effective (ICER=US\$22 623 (US\$22 602 to US\$22 645) per DALY averted) compared with 50% coverage at a cost-effectiveness threshold of US\$919.11.

Under the rapid vaccination scenario, a 30% vaccine coverage strategy was even more cost-effective (ICER=US\$–1607 (US\$–1609 to US\$–1604) per DALY averted compared with no vaccination. The ICERs of 50% and 70% coverage strategies under the rapid scenario are US\$18 257 (US\$18 226 to US\$18 287) and US\$44 250 (US\$44 126 to US\$44 374) per DALY averted compared with 30% and 50% coverage strategies, respectively, and hence are not cost-effective.

Sensitivity analysis

Table 3 presents the univariate sensitivity analysis of under-reporting of hospitalisations and deaths, from a societal perspective. Assuming no under-reporting or adjusting the under-reporting factor to 2, results in all the scenarios having ICERs above the cost-effectiveness threshold, except the 30% coverage with a rapid deployment. On the other hand, with an under-reporting factor of 3 or 4, 30% coverage with a rapid and non-rapid vaccination scenario remained cost saving.

Online supplemental figure S5 summarises the effects of vaccine prices and discounting rates of DALYs on the ICER. Vaccine prices, of the two

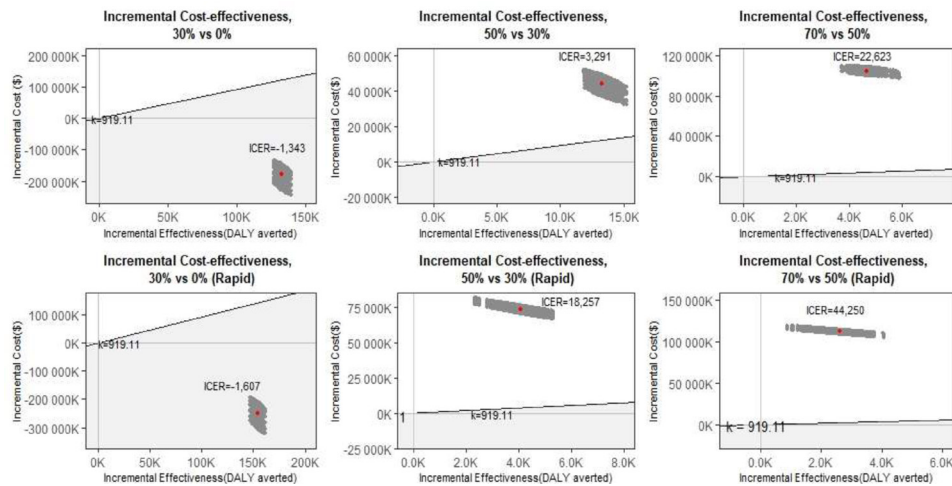


Figure 2 Probabilistic sensitivity analysis of different vaccination strategies from a societal perspective. The first row shows the vaccine scenarios comparisons under a non-rapid roll-out pace while the second row shows the rapid roll-out results. Each grey dot represents a pair of values of incremental cost and incremental effectiveness and the red point is the mean ICER points for each vaccine comparison. The grey shaded area below the diagonal cost-effectiveness threshold line ($k=US\$919.11$) shows the cost-effective region. DALY, disability-adjusted life-year; ICER, incremental cost-effectiveness ratio.

parameters had the largest effect on the ICERs: leading to a 32%–103% decrease and a 36%–77% increase in ICERs across the different vaccination scenarios.

The one-way sensitivity analysis focusing solely on a health system's perspective is presented in online supplemental table S3. When considering this perspective, the total costs across the vaccination strategies increase as coverage increases, as reported from a societal perspective. However, the no vaccination scenario affords the least costs (US\$313million). The reported ICERs increase with increased coverage and the 30% coverage with a non-rapid and rapid vaccination pace are below the threshold: ICER=US\$555 (US\$553 to US\$557) and US\$291 (US\$290 to US\$295) per DALY averted,

respectively, and considered cost-effective from a health system's perspective.

Figure 2 represents the findings of the probabilistic sensitivity analysis from a societal perspective. The region below the cost-effectiveness threshold line and within the grey region, shows all the points that are cost-effective at a cost-effectiveness threshold of US\$919.11. For instance, the dominance of the 30% coverage scenarios (ie, more effectiveness at a lower cost) compared with no vaccination, was shown in 100% of the replications (ie, 100% of the cost-effect pairs were in the southeast quadrant). Further, 100% of the replications for 50% coverage and 70% coverage strategies (both rapid and non-rapid roll-out) were in the northeast quadrant (implying that these strategies were more costly but also more effective

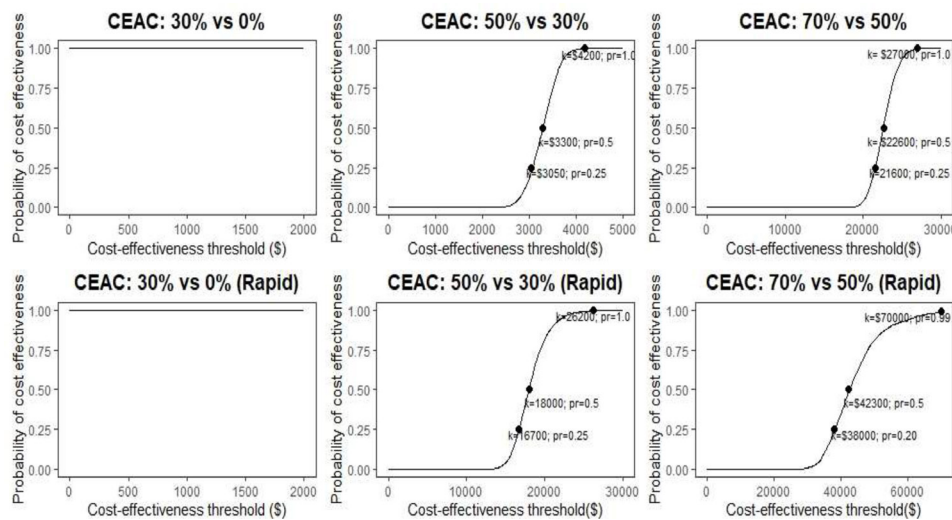


Figure 3 Cost-effectiveness acceptability curves (CEAC) showing the probability that each index scenario is cost-effective compared with the comparator over a range of cost-effectiveness thresholds (k =cost-effectiveness thresholds, pr =probability of cost-effectiveness).

compared with the 30% and 50% coverage strategies, respectively).

Figure 3 presents the cost-effectiveness acceptability curves of the analysis from a societal perspective based on a range of cost-effectiveness thresholds. Under the non-rapid vaccination roll-out and given a US\$3300 willingness to pay threshold, the probability of the 50% coverage strategy being cost-effective compared with 30% coverage would be 0.5. Further, there was 0.5 probability that the 70% coverage in comparison to 50% coverage would be cost-effective at a threshold of US\$22 600 in the non-rapid deployment.

DISCUSSION

We assessed the epidemiological impact and cost-effectiveness of a range of COVID-19 vaccine deployment strategies and scenarios in Kenya. Our findings show that if Kenya had started with a full-scale vaccination programme in September 2021 and with an omicron-like variant introduced in November 2021, the deployment of COVID-19 vaccines in the Kenya population would likely avert a substantial number of cases, hospitalisations and deaths from COVID-19. We find that a strategy to vaccinate mostly older adults (80% of those over 50 years) who are at high risk of severe disease but which achieves low (30%) overall population coverage, yields the greatest reductions in severe infections and deaths per fully vaccinated adult. The marginal health benefits decrease with higher vaccine coverage levels (50% and 70%) as an increasing proportion of low risk younger adults, most with some immunity from previous infection, are vaccinated. These diminishing returns of increased coverage result in only the programme for older adults (ie, the 30% coverage scenario) being cost-effective while the expansion to younger age groups (ie, 50% and 70%) was found not cost-effective. Further, where an upsurge of SARS-CoV-2 occurs shortly after scale-up of vaccination (as modelled in this study) then deployment strategies that achieve rapid coverage of the target groups are more effective compared with slow vaccine deployment strategies.

Our findings are similar to evidence from South Africa, Madagascar, Pakistan, UK and USA that found vaccinating their population would decrease COVID-19 infections and deaths compared with a no vaccination scenario^{11 39–42} and increasing vaccination coverage would increase the clinical benefits.^{39 41} The South African study also found that a rapid vaccination roll-out pace resulted in ‘better’ clinical outcomes (infections and deaths averted) and economic effectiveness compared with a non-rapid roll-out pace.³⁹ The studies done in Madagascar, UK and USA reported a greater impact when distribution of vaccines was prioritised according to the number of people of an older age in the region or among the elderly, reflecting similar findings to our study.^{11 40 42} However, in contrast to the South African and Pakistan studies^{39 41} who found that higher coverage scenarios

had higher marginal impacts, we found that a minimal vaccine coverage of 30% of the adult Kenyan population targeting older age groups had the highest marginal impact. These differences could be explained by differences in the demographic profiles of the different populations of study. Higher population coverage with the COVID-19 vaccines have greater health impacts in countries that have higher proportions of the elderly and/or low previous exposure to COVID-19.

Using a societal perspective (that incorporates health system costs and productivity losses), we find that COVID-19 vaccination in Kenya is most cost-effective when targeted at older age groups in the population. This is because all our scenarios have the elderly covered first, and the incremental impact of increasing vaccination coverage among younger populations was less value for money. Given that the proportion of the elderly population in Kenya is low (11% of total population are aged 50 years and above),⁹ targeting the COVID-19 vaccine to this vulnerable population achieves high cost-effectiveness at relatively low population-level vaccine coverage; 30% coverage of the population ensures that the maximal 80% of the older age group is vaccinated and a very low coverage of the younger age group (19%). Accounting for productivity losses improves the cost-effectiveness profile of COVID-19 vaccines, compared with when only direct health system costs are considered. For instance, for the 30% coverage scenarios with both a non-rapid and rapid deployment pace, the ICERs decreased on average by 342% and 652%, when the societal perspective was considered as opposed to the health system perspective, and as a result improving the cost-effectiveness profile. This underlines the limitations of using a narrow health system perspective that ignores broader societal costs of health system interventions. This is even more so for a vaccine deployed in a pandemic that has substantial socio-economic impacts, in addition to health impacts. These findings mirror cost-effectiveness studies of COVID-19 vaccination done in Turkey and Pakistan that found that although COVID-19 vaccination strategies were cost-effective from a health system’s perspective, they were cost saving from a societal perspective.^{41 43} This is in line with arguments from studies that estimate the public health value and impact of vaccination, which argue the need to broaden the perspectives for cost-effectiveness analysis of vaccines, as their impact is far-reaching, especially in the context of a pandemic.^{44–46}

These findings have implications for COVID-19 vaccination policy in Kenya and other low-income and middle-income countries settings with comparable demographic and COVID-19 epidemiological profiles. First, not unexpectedly, where an outbreak is imminent efforts to rapidly deploy the vaccine not only avert more cases, hospitalisation, and deaths, but are also more cost-effective. By extension, had Kenya been able to deploy vaccines more rapidly, benefits would have been greater. Second, COVID-19 vaccination is likely to offer the best value for money when targeted to older age groups and possibly other vulnerable groups (such

as those with risk increasing comorbidities) with high risk of severe disease and death, rather than to the whole population, in settings with overall low risk of severe disease and deaths, and high natural immunity due to previous exposure. This has several further implications. Kenya and other similar settings will achieve better health impacts and value for money with relatively small numbers of vaccines targeting the high-risk sections of the population. Against a context of constrained fiscal space for health, it is likely more prudent for Kenya and other African countries to target the vulnerable rather than whole populations. This consideration is likely to be even more relevant as African countries consider two shifts; the eligibility of children (below the age of 18 years) to COVID-19 vaccination and the transition to endemicity. If an endemic scenario will require annual vaccinations, Kenya and other African countries are unlikely to afford yearly vaccinations of their entire population. It is also apparent that such a strategy (vaccinating the entire population) is unlikely to be cost-effective, necessitating the need for Kenya and other African countries with comparable demographic and epidemic profiles to be both pragmatic and evidence-based in setting COVID-19 vaccine coverage policies and targets that are both feasible, effective and cost-effective in their contexts (rather than replicating high income country strategies).

These results should be interpreted within the context of several limitations. First, our results are dependent on model assumptions and input parameters, as is the case with all modelling studies. We selected transmission model parameters based on published literature and available observation data. However, some data were limited, lacking or uncertain and therefore we assumed our 'best' estimate for Kenya. For example, we used estimates of vaccine effectiveness based on UK data and assume a duration of 14 days between vaccination and peak efficacy within our model structure. We noted from literature,^{32–35} vaccine effectiveness varies with age, duration between vaccination and testing of efficacy, variant of infection and the type of vaccine among other factors. The model does not consider the different professions of the population such as essential workers (healthcare workers, teachers, among others) as it focusses on age as the key risk group. However, front-line workers may be important to target since preventing infection among them lessens the potential impact on health and learning capacity. The latter might become more influential in the future with new vaccines if they are more effective in preventing re-infection and mild symptoms than current generation of vaccines. Second, sub-Saharan African countries like Kenya have notably reported lower cases and deaths compared with other countries across the globe, this could be attributed to their lower testing capacity. Hence, we assumed an under-reporting factor of 1:5 in hospitalised cases and deaths. Third, we instituted vaccination roll-out near in time to the introduction of a new variant, which enhances the benefit of rapid over slow roll-out. Distance between vaccine introduction and the emergence of an immune escape

variant is likely to favour slower vaccine roll-out. Fourth, assumptions about waning immunity (natural and vaccine) and varying protection depending on variants affect the results. We; therefore, acknowledge the need to further investigate duration of protection accorded by both vaccines and natural immunity. Fifth, at the time of writing this (May 2022—over 1 year after the start of the vaccination campaign in Kenya), only 1% of the adult population had received booster doses.⁴⁷ As a result, we did not include booster doses in this analysis but recognise that their inclusion may change the findings by improving the epidemiological impact of the vaccines as well as increase the costs of the vaccination programme. Sixth, in relation to the economic evaluation, although the cost-effectiveness analysis was conducted from a societal perspective, some costs have not been fully captured due to unavailability of data. These costs include household indirect costs incurred due to COVID-19 illness (eg, transport costs), costs as a result of long-COVID, and reduced productivity for those in the formal sector with asymptomatic/mild disease. In the latter, although we assume that they can resume work from home/places of quarantine they may have reduced productivity which is not captured in this analysis. These costs not captured in the analysis are however expected to be minimal. Seventh, the analysis assumed similar vaccine delivery costs for both rapid and non-rapid vaccination across similar coverage levels. However, it is likely that the rapid vaccination scenario may need more resources, especially cold chain equipment to hold larger batches of vaccines at a time. Eighth, the reported uncertainty of the ICER likely does not capture the full extent of the uncertainty, given the uncertainty of the costs of a yet to be established adult vaccination programme in Kenya. Lastly, the economic evaluation considers a 1.5-year time frame, potentially excluding costs and benefits of COVID-19 that may accrue over a longer period of time.

CONCLUSION

This study contributes to the growing body of literature on the health impact and cost-effectiveness of COVID-19 vaccines. Kenya will achieve both greater marginal health impacts and better value for money if it prioritises a targeted vaccination strategy among those at increased risk of severe disease and at a rapid roll-out speed. The cost-effectiveness of the COVID-19 vaccine should be considered alongside other priority setting considerations in the Kenyan context.

Author affiliations

¹Health Economics Research Unit, KEMRI-Wellcome Trust Research Programme Nairobi, Nairobi, Kenya

²Institute of Healthcare Management, Strathmore University, Nairobi, Kenya

³Kenya Medical Research Institute (KEMRI)-Wellcome Trust Research Programme, Kilifi, Kenya

⁴The Centre for Mathematical Modelling of Infectious Diseases, London School of Hygiene and Tropical Medicine, London, UK

⁵The Zeeman Institute for Systems Biology and Infectious Disease Epidemiology Research (SBIDER), University of Warwick, Coventry, UK

⁶School of Life Sciences, University of Warwick, Coventry, UK

⁷Centre for Tropical Medicine and Global Health, Nuffield Department of Medicine, University of Oxford, Oxford, UK

⁸Ministry of Health, Government of Kenya, Nairobi, Kenya

⁹Presidential Policy & Strategy Unit, The Presidency, Government of Kenya, Nairobi, Kenya

¹⁰Mathematics Institute, University of Warwick, Coventry, UK

Twitter Ambrose Agweyu @AmbroseAgweyu and Edwine Barasa @edwinebarasa

Acknowledgements We would like to acknowledge the Health Intervention and Technology Assessment Program (HITAP) and the Africa CDC Health Economic Program for their advice on the analysis.

Contributors EB, DJN and PB conceptualised the study. SO, JO, CO, AK, RA, MO, AA, GMW, SU, EO, LIO-O, CNA, KK, PA, MM, RAA, WN, IMO, JAGS, PB and EB acquired the data. SPCB, JO, SO and CO analysed the data. SO, JO, SPCB, CO, PB, DJN and EB were involved in the interpretation of the data and work. SO and JO wrote the first draft of the manuscript which was subsequently revised for important intellectual content by all authors. All authors read and approved the final manuscript. EB and DJN are responsible for the overall content as guarantors.

Funding This work was supported by funding from the Bill and Melinda Gates Foundation funded International Decision Support Initiative (IDS), and funding from the National Institute for Health Research (NIHR) Global Health Research Unit on the Application of Genomics and Modelling to the Control of Virus Pathogens (17/63/82), on Mucosal Pathogens (16/136/46), and on Tackling Infections to Benefit Africa (16/136/33), using UK aid from the UK Government to support global health research, The UK Foreign, Commonwealth and Development Office and Wellcome Trust (grant# 220985/Z/20/Z).

Competing interests None declared.

Patient and public involvement Patients and/or the public were not involved in the design, or conduct, or reporting, or dissemination plans of this research.

Patient consent for publication Not applicable.

Ethics approval The KEMRI Scientific and Ethics Review Unit approved this study under KEMRI/SERU/CGMR-C/4244

Provenance and peer review Not commissioned; externally peer reviewed.

Data availability statement Data are available in a public, open access repository. All code and data for the transmission model and economic evaluation analysis underlying this study is accessible at the Github repository: <https://github.com/SamuelBrand1/KenyaCoVaccines>.

Supplemental material This content has been supplied by the author(s). It has not been vetted by BMJ Publishing Group Limited (BMJ) and may not have been peer-reviewed. Any opinions or recommendations discussed are solely those of the author(s) and are not endorsed by BMJ. BMJ disclaims all liability and responsibility arising from any reliance placed on the content. Where the content includes any translated material, BMJ does not warrant the accuracy and reliability of the translations (including but not limited to local regulations, clinical guidelines, terminology, drug names and drug dosages), and is not responsible for any error and/or omissions arising from translation and adaptation or otherwise.

Open access This is an open access article distributed in accordance with the Creative Commons Attribution Non Commercial (CC BY-NC 4.0) license, which permits others to distribute, remix, adapt, build upon this work non-commercially, and license their derivative works on different terms, provided the original work is properly cited, appropriate credit is given, any changes made indicated, and the use is non-commercial. See: <http://creativecommons.org/licenses/by-nc/4.0/>.

ORCID iDs

Stacey Orangi <http://orcid.org/0000-0002-3236-5229>

Angela Kairu <http://orcid.org/0000-0002-0965-4460>

Ambrose Agweyu <http://orcid.org/0000-0001-8760-1279>

Edwine Barasa <http://orcid.org/0000-0001-5793-7177>

REFERENCES

- Mathieu E, Ritchie H, Ortiz-Ospina E. Our World Data. Coronavirus pandemic (COVID-19); 2021. <https://ourworldindata.org/coronavirus> [Accessed 26 May 2022].
- World Health Organization. COVID-19 vaccines, 2021. Available: <https://www.who.int/emergencies/diseases/novel-coronavirus-2019/covid-19-vaccines> [Accessed 20 Oct 2021].
- Taylor L. Covid-19: Hong Kong reports world's highest death rate as zero covid strategy fails. *BMJ* 2022;376:o707.
- Brand SPC, Ojal J, Aziza R, et al. COVID-19 transmission dynamics underlying epidemic waves in Kenya. *Science* 2021;374:989–94.
- Chisale MRO, Ramazanu S, Mwale SE, et al. Seroprevalence of anti-SARS-CoV-2 antibodies in Africa: a systematic review and meta-analysis. *Rev Med Virol* 2022;32:e2271.
- Ministry of Health Kenya. National COVID-19 vaccine deployment plan; 2021.
- Ministry of Health. Kenya COVID-19 vaccination Program-Daily situation report, 2022. Available: <https://www.health.go.ke/wp-content/uploads/2022/03/MINISTRY-OF-HEALTH-KENYA-COVID-19-IMMUNIZATION-STATUS-REPORT-20TH-MARCH-2022.pdf> [Accessed 22 Mar 2022].
- World Bank. World bank open data, 2021. Available: <https://data.worldbank.org/> [Accessed 11 Nov 2021].
- Kenya National Bureau of Statistics. 2019 Kenya population and housing census: volume III, 2019.
- Ministry of Health. COVID-19 outbreak in Kenya. daily situation report; 2022 [Accessed 25 May 2022].
- Moore S, Hill EM, Dyson L, et al. Modelling optimal vaccination strategy for SARS-CoV-2 in the UK. *PLoS Comput Biol* 2021;17:e1008849.
- Moore S, Hill EM, Tildesley MJ, et al. Vaccination and non-pharmaceutical interventions for COVID-19: a mathematical modelling study. *Lancet Infect Dis* 2021;21:793–802.
- Uyoga S, Adetifa IMO, Otiende M, et al. Prevalence of SARS-CoV-2 antibodies from a national serosurveillance of Kenyan blood donors, January–March 2021. *JAMA* 2021;326:1436–8.
- Etyang AO, Adetifa I, Omoro R. SARS-CoV-2 seroprevalence in three Kenyan health and demographic surveillance sites, December 2020–May 2021. *medRxiv* 2022.
- Rees EM, Nightingale ES, Jafari Y, et al. COVID-19 length of hospital stay: a systematic review and data synthesis. *BMC Med* 2020;18:270.
- UK Health Security Agency. COVID-19 vaccine surveillance report: week 11, 2022. Available: https://assets.publishing.service.gov.uk/government/uploads/system/uploads/attachment_data/file/1061532/Vaccine_surveillance_report_-_week_11.pdf [Accessed 06 Apr 2022].
- Clifford S, Waight P, Hackman J. Effectiveness of BNT162b2 and ChAdOx1 against SARS-CoV-2 household transmission: a prospective cohort study in England. *medRxiv* 2021.
- Keeling MJ, Thomas A, Hill EM. Waning, boosting and a path to endemicity for SARS-CoV-2. *medRxiv* 2021.
- Townsend JP, Hassler HB, Wang Z, et al. The durability of immunity against reinfection by SARS-CoV-2: a comparative evolutionary study. *Lancet Microbe* 2021;2:e666–75.
- Drummond M, Sculpher M, Claxton K. *Methods for the economic evaluation of health care programmes*. Fourth Edition. Oxford: Oxford University Press, 2015.
- Johns B, Baltussen R, Hutubessy R. Programme costs in the economic evaluation of health interventions. *Cost Eff Resour Alloc* 2003;1:1–10.
- Orangi S, Kairu A, Ngatia A, et al. Examining the unit costs of COVID-19 vaccine delivery in Kenya. *BMC Health Serv Res* 2022;22.
- Barasa E, Kairu A, Ng'ang'a W, et al. Examining unit costs for COVID-19 case management in Kenya. *BMJ Glob Health* 2021;6:e004159.
- Pritchard C, Sculpher M. *Productivity costs: principles and practice in economic evaluation*, 2000.
- Fox-Rushby JA, Hanson K. Calculating and presenting disability adjusted life years (DALYs) in cost-effectiveness analysis. *Health Policy Plan* 2001;16:326–31.
- World Health Organization. Life tables: Kenya. Glob. heal. Obs. data Repos; 2020. <https://apps.who.int/gho/data/view.main.60850?lang=en> [Accessed 20 Oct 2021].
- Luangasanatip N, Prawjaeng J, Saralamba S. Optimal vaccine strategy to control COVID-19 pandemic in middle-income countries: modelling case study of Thailand. *Res Sq* 2021.
- Salomon JA, Haagsma JA, Davis A, et al. Disability weights for the global burden of disease 2013 study. *Lancet Glob Health* 2015;3:e712–23.
- Haagsma JA, Maertens de Noordhout C, Polinder S, et al. Assessing disability weights based on the responses of 30,660 people from four European countries. *Popul Health Metr* 2015;13:10.
- Ochalek J, Lomas J, Claxton K. Estimating health opportunity costs in low-income and middle-income countries: a novel approach and evidence from cross-country data. *BMJ Glob Health* 2018;3:e000964.

- 31 Woods B, Reville P, Sculpher M, *et al.* Country-level cost-effectiveness thresholds: initial estimates and the need for further research. *Value Health* 2016;19:929–35.
- 32 Voysey M, Costa Clemens SA, Madhi SA, *et al.* Single-dose administration and the influence of the timing of the booster dose on immunogenicity and efficacy of ChAdOx1 nCoV-19 (AZD1222) vaccine: a pooled analysis of four randomised trials. *Lancet* 2021;397:881–91.
- 33 Eyre DW, Taylor D, Purver M. The impact of SARS-CoV-2 vaccination on alpha & delta variant transmission. *medRxiv* 2021.
- 34 Ioannou GN, Locke ER, O'Hare AM, *et al.* COVID-19 vaccination effectiveness against infection or death in a national U.S. health care system : a target trial emulation study. *Ann Intern Med* 2022;175:352–61.
- 35 Sheikh A, Robertson C, Taylor B. BNT162b2 and ChAdOx1 nCoV-19 vaccine effectiveness against death from the delta variant. *N Engl J Med* 2021;385:2195–7.
- 36 Tembo J, Maluzi K, Egbe F, *et al.* Covid-19 in Africa. *BMJ* 2021;372:n457.
- 37 Saltelli A, Annoni P, Azzini I, *et al.* Variance based sensitivity analysis of model output. design and estimator for the total sensitivity index. *Comput Phys Commun* 2010;181:259–70.
- 38 Orangi S, Ojal J, Brand SP. Data from: epidemiological impact and cost-effectiveness analysis of COVID-19 vaccination in Kenya GitHub Repos; 2022. <https://github.com/SamuelBrand1/KenyaCoVaccines> [Accessed 02 Jun 2022].
- 39 Reddy KP, Fitzmaurice KP, Scott JA, *et al.* Clinical outcomes and cost-effectiveness of COVID-19 vaccination in South Africa. *Nat Commun* 2021;12:6238.
- 40 Moghadas SM, Vilches TN, Zhang K, *et al.* The impact of vaccination on coronavirus disease 2019 (COVID-19) outbreaks in the United States. *Clin Infect Dis* 2021;73:2257–64.
- 41 Pearson CAB, Bozzani F, Procter SR, *et al.* COVID-19 vaccination in sindh province, Pakistan: a modelling study of health impact and cost-effectiveness. *PLoS Med* 2021;18:e1003815.
- 42 Rasambainarivo F, Ramiadantsoa T, Raheerinandrasana A, *et al.* Prioritizing COVID-19 vaccination efforts and dose allocation within madagascar. *BMC Public Health* 2022;22:724.
- 43 Hagens A, İnkaya Ahmet Çağkan, Yildirak K, *et al.* COVID-19 vaccination scenarios: a cost-effectiveness analysis for turkey. *Vaccines* 2021;9. doi:10.3390/vaccines9040399. [Epub ahead of print: 18 04 2021].
- 44 Gessner BD, Kaslow D, Louis J, *et al.* Estimating the full public health value of vaccination. *Vaccine* 2017;35:6255–63.
- 45 Wilder-Smith A, Longini I, Zuber PL, *et al.* The public health value of vaccines beyond efficacy: methods, measures and outcomes. *BMC Med* 2017;15:1–9.
- 46 Rodrigues CMC, Plotkin SA. Impact of vaccines; health, economic and social perspectives. *Front Microbiol* 2020;11:1526.
- 47 Ministry of Health. Kenya COVID-19 vaccination Program-Daily situation report: 25th may 2022, 2022. Available: <https://www.health.go.ke/wp-content/uploads/2022/05/MINISTRY-OF-HEALTH-KENYA-COVID-19-IMMUNIZATION-STATUS-REPORT-24TH-MAY-2022.pdf> [Accessed 26 May 2022].

Supplementary file – Reflexivity Statement

Study Conceptualisation

1. How does this study address local research and policy priorities?

This study was co-produced by the KEMRI-Wellcome Trust, a research organization in Kenya and the Ministry of Health (MOH) Kenya, based on a need expressed by the MOH for evidence to inform the country's COVID-19 response. Co-authors KK, PA, WN, MM, RA are policy makers based at the MOH. The study specifically addresses the singled-out country priority for evidence to inform its COVID-19 vaccination strategy.

2. How were local researchers involved in study design?

The design of this study was primarily led by local researchers with EB as the senior researcher, and SO and JO leading the implementation of the design by developing the economic and epidemiological models respectively.

Research management

1. How has funding been used to support the local research team?

Funding for this work has supported SO's PhD studentship, and CO's post-doctoral training, both based at the KEMRI-Wellcome Trust Research Programme. SO's PhD studentship is supervised by EB & JO, while CO's post-doctoral training is supervised by JN.

Data acquisition and analysis

1. How are research staff who conducted data collection acknowledged?

All research staff that conducted data collection for this work have also been involved in the analysis of the data and manuscript writing and have hence been included as co-authors.

2. Do all members of the research partnership have access to study data?

All members of the partnership have access to data.

3. How was data used to develop analytical skills within the partnership?

SO and CO, both based at KEMRI-Wellcome have developed analytical skills in cost-effectiveness analysis using dynamic transmission models. Research members have worked collaboratively as a modelling team facilitating the sharing of skills across the multidisciplinary team members.

Data interpretation

1. How have research partners collaborated in interpreting study data?

Research partners have set up a modelling team led by KEMRI-Wellcome Trust, that formally holds working meetings twice a week. These meetings have been used to jointly formulate research questions, deliberate and agree on analytical approaches, provide support implement the agreed on analytical approach, to provide internal review of preliminary analytical outputs, and contribute to manuscript writing.

Drafting and revising for intellectual content

1. How were research partners supported to develop writing skills?

The research team is comprised of several senior scientists with established writing skills. These scientists worked with earlier career staff to support the writing.

2. How will research products be shared to address local needs?

Findings from this analysis have been disseminated locally, regionally, and internationally through presentations, and have been shared with MOH policy makers in the form of a policy brief. There has also been media engagement.

Authorship**1. How is the leadership, contribution and ownership of this work by LMIC researchers recognised within the authorship?**

The majority of the co-authors in this manuscript are LMIC researchers. The joint lead authors (SO and JO), as well as the senior author (EB) are all LMIC researchers.

2. How have early career researchers across the partnership been included within the authorship team?

The authorship team includes several early career researchers. SO (who is the lead author), AK, and MO are PhD students.

3. How has gender balance been addressed within the authorship?

Eight authors (SO, CO, AK, RA, SU, LOO, MM, WN) are female, while 17 are male

Training**1. How has the project contributed to training of LMIC researchers?**

Funding for this work has supported SO's PhD studentship, and CO's post-doctoral training, both based at the KEMRI-Wellcome Trust Research Programme. SO's PhD studentship is supervised by EB & JO, while CO's post-doctoral training is supervised by JN. This project has been part of the training for SO and CO.

Infrastructure**1. How has the project contributed to improvements in local infrastructure?**

This project has not directly contributed to improvements in local infrastructure.

Governance**1. What safeguarding procedures were used to protect local study participants and researchers?**

There was no primary data collection as part of this project, therefore this question is not directly applicable.

SUPPLEMENTARY INFORMATION

Transmission model

Transmission model overview

The dynamics of SARS-CoV-2 transmission in each of the 47 Kenyan counties were assumed to follow a dynamic model adapted from a previous model;^[1] here we extend the (modified SEIRS type) transmission model structure to include age stratification and vaccination. The epidemiological dynamics in each county are described by the following system of differential equations:

$$\begin{aligned}
 \frac{dS_{a,v}}{dt} &= -\sigma_a S_{a,v} (1 - \pi_v^{sus}) \lambda_a + \rho_{a,v-1} S_{a,v-1} - \rho_{a,v} S_{a,v} \\
 \frac{dE_{a,v}}{dt} &= \sigma_a (S_{a,v} + \sigma_{\omega 1} W1_{a,v} + \sigma_{\omega 2} W2_{a,v}) (1 - \pi_v^{sus}) \lambda_a - \alpha E_{a,v} + \rho_{a,v-1} E_{a,v-1} - \rho_{a,v} E_{a,v} \\
 \frac{dA_{a,v}}{dt} &= \alpha E_{a,v} (1 - \delta_a) - \gamma_A A_{a,v} + \rho_{a,v-1} A_{a,v-1} - \rho_{a,v} A_{a,v} \\
 \frac{dP_{a,v}}{dt} &= \alpha E_{a,v} \delta_a - \alpha_P P_{a,v} + \rho_{a,v-1} P_{a,v-1} - \rho_{a,v} P_{a,v} \\
 \frac{dD_{a,v}}{dt} &= \alpha_P P_{a,v} - \gamma_D D_{a,v} + \rho_{a,v-1} D_{a,v-1} - \rho_{a,v} D_{a,v} \\
 \frac{dR_{a,v}}{dt} &= \gamma_A A_{a,v} + \gamma_M M_{a,v} + \gamma_V V_{a,v} - \omega R_{a,v} + \rho_{a,v-1} R_{a,v-1} - \rho_{a,v} R_{a,v} \\
 \frac{dW1_{a,v}}{dt} &= \omega_1 R_{a,v} - \sigma_{\omega} \sigma_a W1_{a,v} (1 - \pi_v^{sus}) \lambda_a - \omega_2 W1_{a,v} + \rho_{a,v-1} W1_{a,v-1} - \rho_{a,v} W1_{a,v} \\
 \frac{dW2_{a,v}}{dt} &= \omega_2 W1_{a,v} - \sigma_a W2_{a,v} (1 - \pi_v^{sus}) \lambda_a + \rho_{a,v-1} W2_{a,v-1} - \rho_{a,v} W2_{a,v}
 \end{aligned}
 \tag{Equation 1}$$

The state variables are: Susceptible (**S**), latently infected (**E**), asymptotically infectious (**A**), pre-symptomatic infectious (**P**), symptomatic/diseased infectious (**D**), recovered and temporarily immune (**R**), and previously recovered/immune whose immunity to reinfection has waned (**W1**) before disappearing (**W2**). The indexing variables are age (*a*) and vaccination dose status (*v*), see below for further details on index variable structure. The age-specific force of infection was denoted λ_a (see below for details). The rate of progressing through latent uninfected stage (α), pre-symptomatic infectious state (α_P), rate of loss of complete immunity in two stages (ω_1 , ω_2), and the decreased susceptibility due to prior infection in stage **W1** (σ_{ω}), were assumed to be identical for all age groups, vaccination statuses, prior infection events, and eventual severity of the infection episode. The recovery rates (γ_A , γ_D) depended on the severity of the episode, but not other factors. The baseline susceptibility per infectious contact (σ_a) and probability of developing symptoms (δ_a), were assumed to depend on the age of the individuals. π_v^{sus} gives the effectiveness of vaccine status *v* at blocking transmission per infectious contact (see below). The per-capita rate at which a person in age group *a* and with vaccine status *v* transitioned to their next vaccine status was denoted $\rho_{a,v}$ (see below). Supplementary figure 1 gives a visual overview of the model dynamics.

1

1

Age structure for transmission model

In this paper we used a coarse-grained set of age indices, partly to reduce number of model compartments and thereby increase the efficiency of parameter estimation (see below), and also partly because the data used in parameter estimation did not support a finer grained age index. The six age groups corresponding to the age indices $a = 1, \dots, 6$ were 0-19, 20-49, 50-59, 60-69, 70-79 and 80+ year olds. When using more fine-grained age-specific data we used population weighted average values over the finer age group categories within each of the coarser six age groups used in this model to generate data. The data we used in the transmission model which was translated from a larger number of age groups to the six used in this model was as following:

- Age- and setting- specific contact rates for Kenya from Prem and Jit.[2] These are provided in 16 5-year age groups and 75+ year olds.
- Age-specific relative susceptibility to infection (σ_a). These were accessed from UK focused modelling and analysis.[3] (Supplementary figure 2)
- Age-specific chance of a symptomatic episode given infection (δ_a). These were accessed from UK focused modelling and analysis.[3] (Supplementary figure 2)

Vaccine status and vaccination effects on transmission model dynamics and waning vaccination dynamics

We used five vaccination statuses to index individuals: unvaccinated ($v = 1$), vaccinated with one ($v = 2$) or two doses ($v = 3$) with sufficient time elapsed since dose inoculation that maximum vaccine efficacy had been achieved (assumed to be 14 days), and two stages of waned vaccination ($v = 4, 5$). The vaccination waning dynamics follow those described by Keeling et al.[4]

Vaccine status acted on the dynamics of the model in four distinct ways:

- 1) Decreasing the chance of infection per infectious contact by a factor $1 - \pi_v^{sus}$ where π_v^{sus} was the effectiveness of vaccine dose status v at reducing infection.
- 2) Decreasing the probability of severe disease after infection by a factor $1 - \pi_v^{dis}$ where π_v^{dis} was the effectiveness of vaccine dose status v against severe disease.
- 3) Decreasing the probability of death after infection by a factor $1 - \pi_v^{death}$ where π_v^{death} was the effectiveness of vaccine dose status v against death.
- 4) Decreasing the infectiousness of dosed infecteds by a factor $1 - \pi_v^{inf}$ where π_v^{inf} was the effectiveness of vaccine dose status v against transmitting infection.

We follow the “VE \rightarrow 0%” scenario from Keeling et al,[4] where the effectiveness of the vaccine against acquisition of COVID-19 and infectiousness during a COVID-19 episode eventually decreases to zero ($\pi_5^{sus} = 0, \pi_5^{inf} = 0$), whilst the eventual effectiveness against severe disease and death decreases to 70% ($\pi_5^{dis} = \pi_5^{death} = 0.7$). The pre-waned vaccination status ($v = 4$) has the same vaccine effectiveness as full second dose vaccination status ($v = 3$) but is used to give non-exponential waning rates over an average of 430 days for both stages of waning vaccine effectiveness. Therefore, the per-capita transition rates $\rho_{a,v}$ in equation 1 divide into:

$$\rho_{a,v} = \begin{cases} 0, & v = 0 \\ v_{a,v}, & v = 1,2 \\ \xi_1, & v = 3 \\ \xi_2, & v = 4 \\ 0, & v = 5 \end{cases} \quad \text{Equation 2}$$

Where $v_{a,1}$ and $v_{a,2}$ are the per-capita daily rates at which individuals in age group a receive their first and second doses of vaccine, and $\xi_1 = \xi_2 = 2/430$ per day are the waning immunity rates of vaccine effectiveness.

Although, this model choice closely follows Keeling et al,[4] it should be noted that unlike Keeling et al we assume that protection from vaccines and natural infection combine favorably whereas in Keeling et al it was assumed that protection from natural infection dominated vaccine protection.

Force of infection for transmission model

We define the age-dependent force of infection (λ_a) in three steps. First, we define the effective number of infected in each age group b ,

$$I_b = \sum_v (1 - \pi_v^{inf}) (\epsilon A_{b,v} + P_{b,v} + D_{b,v}) + I_{ext,b}. \quad \text{Equation 3}$$

The effective number of infecteds is the total number rescaled by decreased levels of infectiousness, such as the relatively lower infectiousness of asymptomatic infecteds compared to pre- and post-symptomatic infecteds (ϵ). $I_{ext,b}$ represented an external coupling with infectious people external to internal transmission dynamics. We chose $I_{ext,b}$ such that $\sum_b I_{ext,b} = 100$. Second, the rate of infectious contacts from an effective infected in age group b to anyone in age group a was defined as,

$$T_{ab} = \frac{\beta_0(t) (\beta_{home} T_{ab}^{home} + \beta_{school}(t) T_{ab}^{school} + \beta_{work} T_{ab}^{work} + \beta_{other} T_{ab}^{other})}{N_a}. \quad \text{Equation 4}$$

Contacts occur in any of four main settings: at home, at school, at work or in some other social setting, each of which has an age-specific contact rate matrix for Kenya ($T_{ab}^{home}, T_{ab}^{school}, T_{ab}^{work}, T_{ab}^{other}$) estimated by Prem and Jit.[2] Google mobility data[5] and previous epidemic modelling in Kenya [1] suggest that contact rates in Kenya had returned to approximately pre-pandemic baseline by January 2021, therefore, we treated the setting specific transmission rates per contact for at home, at work and other social setting ($\beta_{home}, \beta_{work}, \beta_{other}$) as constant. Transmission rate per contact at schools ($\beta_{school}(t)$) was constant during term time, but dropped to zero during Kenyan school holidays (19th March – 10th May, 16th July – 26th July, 1st October – 11th October, 23rd December – 4th January). The baseline transmission rate per contact ($\beta_0(t)$) varied according to the SARS-CoV-2 variant frequency in the county (see below). Third, the force of infection was defined as,

$$\lambda_a = \sum_b T_{ab} I_b. \quad \text{Equation 5}$$

Alpha, Beta and Delta variant frequency effect on transmission model dynamics

The Alpha, Beta and Delta variants of SARS-CoV-2 have circulated in Kenya,[6] displaying a pattern of sequential dominance. From December 2020, Alpha and Beta variants increased in frequency [7] with

a complex spatial pattern of relative frequency of Alpha vs Beta within Kenya.[7] Then, from May 2021, the frequency of Delta variant increased very rapidly to complete domination across Kenya.

We modelled the effect of variant frequency on the baseline transmission rate per infectious contact $\beta_0(t)$ as a sequence of strain dominations each occurring over a timescale set by a logistic growth curve,

$$\beta_0(t) = \beta_{wt} [1 + R_{\alpha\beta} \text{logistic}(t; r_{\alpha\beta}, T_{\alpha\beta})] [1 + R_{\delta} \text{logistic}(t; r_{\delta}, T_{\delta})]. \quad \text{Equation 6}$$

Where $\text{logistic}(t; r, T) = \frac{\exp(r(t-T))}{1 + \exp(r(t-T))}$. In this model, β_{wt} is the baseline transmission rate per infectious contact of the origin strain(s), called wild-type strains, circulating in Kenya before Alpha and Beta variants, $(1 + R_{\alpha\beta})$ is the proportional change in the reproductive number for SARS-CoV-2 after domination by Alpha or Beta variant relative to wild-type strains, and $(1 + R_{\delta})$ is the proportional change in the reproductive number for SARS-CoV-2 after domination by Delta variant relative to Alpha or Beta variant. $r_{\alpha\beta}, r_{\delta}, T_{\alpha\beta}, T_{\delta}$ set the exponential rates and timing of the logistic growth curves. The implied relative frequencies of wild-type, Alpha/Beta and Delta variants over time are,

$$\begin{aligned} f_{wt}(t) &= [1 - \text{logistic}(t; r_{\alpha\beta}, T_{\alpha\beta})] [1 - \text{logistic}(t; r_{\delta}, T_{\delta})], \\ f_{\alpha\beta}(t) &= \text{logistic}(t; r_{\alpha\beta}, T_{\alpha\beta}) [1 - \text{logistic}(t; r_{\delta}, T_{\delta})], \\ f_{\delta}(t) &= \text{logistic}(t; r_{\delta}, T_{\delta}). \end{aligned} \quad \text{Equation 7}$$

Transmission model observables: Proportions PCR test and serology test positive

The underlying transmission of SARS-CoV-2 is not observed, rather we have access to swab tests and serological tests (positive and negative) aggregated by date, age, and county. The chance infected individuals test positive for either type of test depends on the number of days post-infection. Therefore, we coupled the dynamics cumulative infections to transmission model,

$$\begin{aligned} \frac{dF_{a,v}}{dt} &= \sigma_a S_{a,v} (1 - \pi_v^{sus}) \lambda_a, \\ \frac{dC_{a,v}}{dt} &= \sigma_a (S_{a,v} + \sigma_{\omega} W1_{a,v} + W2_{a,v}) (1 - \pi_v^{sus}) \lambda_a, \\ \frac{d\bar{C}_{a,v}}{dt} &= \sigma_a (S_{a,v} + 0.5\sigma_{\omega} (1 - \pi_5^{dis}) W1_{a,v} + (1 - \pi_5^{dis}) W2_{a,v}) (1 - \pi_v^{sus}) \lambda_a. \end{aligned} \quad \text{Equation 8}$$

Where $F_{a,v}(t)$ and $C_{a,v}(t)$ were the cumulative number of people in the county in age group a and vaccine status v infected by time t , respectively split by it being their first infection episode or any infection episode. $\bar{C}_{a,v}(t)$ was the reinfection disease risk-weighted cumulative infection rate; that is the total infections discounted by the decreased risk of severe disease among reinfections (see below for use of this observable). In the absence of other evidence, we follow Keeling et al[4] in assuming that protection against disease due to prior infection is similar to that of vaccination. For the fully waned immunity post-natural infection state (**W2**) we assume that the protection from disease is equivalent to fully waned vaccine protection, and, for the partially waned immunity post-natural infection state (**W1**) that this protection is halved relative to **W2**.

The daily new infections, on each day n starting at $t = n$ are then,

$$\begin{aligned} \iota_{F,a,v}(n) &= F_{a,v}(n+1) - F_{a,v}(n), \quad n = 1, 2, \dots \\ \iota_{C,a,v}(n) &= C_{a,v}(n+1) - C_{a,v}(n), \quad n = 1, 2, \dots \end{aligned} \quad \text{Equation 9}$$

The probability that an infected individual would be determined as having been infected τ days after infection if tested by either a PCR swab test or a serology test were denoted, respectively, $Q_{PCR}(\tau)$ and $Q_{sero}(\tau)$. We used the same Q_{PCR} and Q_{sero} probabilities as in Brand et al 2021.[1]

By combining the underlying infection processes and the delay between infection and observability in our available data sets we find that the number of people who would test positive on each day n in each county with either a PCR test ($P_a^+(n)$), or a serology test ($S_a^+(n)$), was,

$$\begin{aligned} P_a^+(n) &= \sum_{s=1}^{n-1} \sum_v \iota_{C,a,v}(s) Q_{PCR}(n-s), \\ S_a^+(n) &= \sum_{s=1}^{n-1} \iota_{F,a,1}(s) Q_{sero}(n-s) + p_{FP} \sum_v S_{a,v}(t). \end{aligned} \quad \text{Equation 10}$$

where t was the midpoint of day n .

p_{FP} was the false positive rate for the serology assay (see supplementary table 1). Underlying assumptions for equation 10 are: 1) that the PCR test is 100% specific to SARS-CoV-2, 2) that only the first infection contributes to the serological status of individuals, but that reinfections contribute to PCR status equally to first infections, and 3) that during the period of transmission parameter inference there were effectively zero vaccinated individuals, and therefore, all seropositivity was evidence of prior nature infection. We do not use any serological data from Kenya after May 2021 when the vaccination rate was very low in Kenya, and, therefore, vaccinations have negligible effect on prevalence of SARS-CoV-2 specific antibodies.

The number of people PCR positive is not observed directly, but rather test positive and negative swab test samples. We consider the *proportion* of these daily samples that are positive to be a potentially biased sample of the true underlying proportion that would be PCR-positive if everyone was tested ($\sum_a P_a^+ / \sum_a N_a$). Therefore, we model the expected proportion PCR test positive (over all age groups) on day n as,

$$\bar{P}^+(n) = \frac{\chi \sum_a P_a^+(n)}{(\chi - 1) \sum_a P_a^+(n) + N}. \quad \text{Equation 11}$$

Where χ is an observed swab sample bias parameter, where $\chi = 1$ indicates unbiased sampling, $\chi < 1$ indicates bias in favour finding PCR negative individuals (i.e., $\bar{P}^+(n) < \sum_a P_a^+ / \sum_a N_a$), and $\chi > 1$ indicates bias in favour of finding PCR positive individuals (i.e., $\bar{P}^+(n) > \sum_a P_a^+ / \sum_a N_a$).

Clinical outcome model

Clinical outcomes of SARS-CoV-2 infections

Severe infections eventually lead to a clinical outcome. We consider three possibilities in this model:

- 1) **Deadly outcome.** Deadly infected individuals die after a delay period defined by the probability distribution f_μ . Death, conditional on infection, occurs with probability μ_a^D .
- 2) **Critical outcome.** Critically infected individuals require a stay in ICU for a duration defined by the probability distribution f_{ICU} , then move to a general ward in a hospital or health facility,

where they stay for a duration defined by the probability duration f_{hosp} . Critical disease, conditional on infection, occurs with probability μ_a^C .

- 3) Severe outcome. Severely infected individuals require a stay in a general ward in a hospital or health facility, where they stay for a duration defined by the probability duration f_{hosp} . Severe disease, conditional on infection, occurs with probability μ_a^S .

Clinical outcome model observables: Reported incidence of deaths, occupancy of general wards and Intensive care units

Incidence rate of clinical outcomes. The lag between infection and needing treatment, for those infected individuals who die, was defined as the convolution of two time-duration distributions:

1. The duration of time between infection and symptoms (days), which we assumed was distributed $LogNormal(\widehat{\log\mu} = 1.64, \widehat{\logstd} = 0.36)$. [8]
2. The duration of time between initial symptoms and severe symptoms (days), sufficient to seek hospitalisation, which we assumed was distributed $U(1,5)$. [9]

We discretized the two distributions to give probability functions f_{IS} for the number of days between infection and symptoms, and f_{SH} for the number of days between symptom onset and severe symptom onset. The probability function for the (discrete) number of days between infection and severe or critical disease, for those who died, f_{dis} , was given as a discrete convolution over these probability mass functions:

$$f_{dis}(\tau) = [f_{IS} * f_{SH}](\tau) \text{ for the probability that severe or critical disease leads to seeking medical assistance } \tau \text{ days after infection, conditional on that as outcome.} \quad \text{Equation 12}$$

We use this delay distribution to give a rate of people in age group a requiring medical treatment on day n up to some unknown age-dependent and variant-dependent risk-factor, which will fit against available data on reported severe, critical and deadly outcomes,

$$l_{dis,a,v,r}(n) \propto \sum_{s < n} f_r(s) [\bar{c}_{a,v}(s+1) - \bar{c}_{a,v}(s)] f_{dis}(n-s). \quad \text{Equation 13}$$

Where $f_r(s)$ is the relative frequency of variant r on day s (see equation 7). Note that in equation (13) the reduction in risk due to reinfection is already accounted for (see equation 8).

Observation of incidence of deadly outcome of infection. There is likely to be under-reporting of deaths due to COVID-19 in Kenya. [10,11] In this paper, we don't have sufficient data to estimate the true level of under-reporting of deaths in Kenya. However, by assuming that the age-dependent risk of death after infection with SARS-CoV-2 is the same in every county, we can estimate county-specific under-reporting/change in risk relative to the capital Nairobi. Concretely, we model the expected number of observed deaths on each day n , in each age group a , and each county c , as,

$$Deaths_{a,c}(n) = \psi_c \mu_a^D \sum_{s < n} \sum_v \sum_r \psi_r^D (1 - \pi_v^{death}) l_{dis,a,v,r}(s) f_\mu(n-s). \quad \text{Equation 14}$$

Where ψ_c is the county-specific under-reporting rate with $\psi_{nairobi} = 1$, ψ_r^D is the relative risk of death by variant with $\psi_{wt}^D = 1$, and the duration of time between needing treatment and death had probability distribution f_μ .

Observation of hospital and ICU occupancy due to severe or critical infections. We don't have access to reports on the incidence of severe and critical cases arriving at hospitals/health facilities and ICUs;

the relevant observables from the clinical outcome model are occupancies of patients overall in Kenya by setting rather than arrival of patients at those settings.

The probability distributions for length of stay in either hospital/health facility or ICU are denoted as f_{hosp} and f_{ICU} , implying upper distribution functions $Q_{hosp}(n) = \sum_{s>n} f_{hosp}(s)$ and $Q_{ICU}(n) = \sum_{s>n} f_{ICU}(s)$ for the probability that a stay in hospital or ICU is longer than n days. The expected total number of people in intensive care units on day n is,

$$ICU(n) = \sum_{a,c} \psi_c \mu_a^C \sum_{s<n} \sum_v \sum_r \psi_r^C (1 - \pi_v^{dis}) l_{dis,a,v,r}(s) Q_{ICU}(n-s). \quad \text{Equation 15}$$

Where ψ_r^C is the relative risk of critical disease by variant with $\psi_{wt}^C = 1$. After a critical case has completed a stay in an ICU, we model them as having a stay in a general ward with the same distribution of length as per a severe case admitted to a general ward (without a stay in ICU). The upper distribution function for the whole stay in ICU and general ward is then $Q_{ICUH}(n) = \sum_{s>n} [f_{ICU} * f_{hosp}](s)$, giving the expected number of critical cases in either ICU or general ward as,

$$ICUH(n) = \sum_{a,c} \psi_c \mu_a^C \sum_{s<n} \sum_v \sum_r \psi_r^C (1 - \pi_v^{dis}) l_{dis,a,v,r}(s) Q_{ICUH}(n-s). \quad \text{Equation 16}$$

The expected number of patients occupying general wards is the addition of severe cases who have been admitted directly to general wards, and critical cases who have completed their stay in ICU and are now in general wards,

$$HOSP(n) = [ICUH(n) - ICU(n)] + \sum_{a,c} \psi_c \mu_a^S \sum_{s<n} \sum_v \psi_r^S (1 - \pi_v^{dis}) l_{dis,a,v,r}(s) Q_{hosp}(n-s). \quad \text{Equation 17}$$

Where ψ_r^S is the relative risk of severe disease by variant with $\psi_{wt}^S = 1$.

Parameter Inference

In this work, we make inferences on two groups of parameters:

1. The parameters of the transmission model in [equations 1-5], and the bias parameter (χ) for the observed versus actual proportion PCR positive in daily swab test [equation (11)].
2. The parameters of the clinical outcome model [equations 12-15]: the relative under-reporting rate by Kenyan county ψ_c , the age-dependent clinical outcome probabilities $\mu_a^S, \mu_a^C, \mu_a^D$, and the variant specific clinical outcome probabilities $\psi_r^D, \psi_r^C, \psi_r^S$.

For the transmission model parameters, we used Bayesian inference to infer a joint posterior distribution for the parameters for each county. For the clinical outcome model, we inferred parameters by minimizing the divergence between model prediction of the observables [equations 14-15 and 17] and actual reporting, under the assumption that the rate of people arriving for medical treatment, up to the unknown risk factors [equation 13], was that implied by the posterior mean prediction implied by the Bayesian inference of the transmission model parameters.

A challenge with using the linelist data in Kenya for inference of transmission was that the metadata concerning the reason for receiving a swab test, the levels of symptoms of people who tested positive,

and their healthcare outcomes were often missing. Overall, more than 90% of the people who tested positive in Kenya, and for whom we have a description of their symptoms, reported no symptoms (asymptomatic). Therefore, unlike model-based inference for COVID-19 transmission in high-income countries we didn't use severe outcomes such as hospitalization or death as data sources for inference, e.g., [12–14] because this data was unreliable. Instead, we concentrated on fitting to the proportion positive of daily swabs test and serological tests jointly with detection rate of cases (see **Transmission model observables: Proportions PCR test and serology test positive** above). It should be noted that this meant that we didn't use age-specific PCR test data, but rather fitted to the aggregate proportion positive over all age groups. However, we did use age-specific seroprevalence data.

We describe the three main ingredients for our Bayesian approach below: 1) the log-likelihood function for the data given a set of parameters, 2) the county-specific hierarchy of prior distributions for the parameters, and, 3) the Markov-chain Monte Carlo method used to draw parameter sets from the posterior distribution.

Bayesian inference of transmission model parameters

Data and log-likelihood function for transmission model. Given the daily PCR and serology data for a county,

$$\mathcal{D}_c = \{ObsS_a^+(n), ObsS_a^-(n), ObsP^+(n), ObsP^-(n)\}_{a=1,\dots,6; n=1,2,3,\dots} \quad \text{Equation 18}$$

The log-likelihood function for the unknown transmission parameters (θ_{TM}) in that county was,

$$l(\theta_{TM}) = P(\mathcal{D}_c | \theta_{TM}) = \sum_n \ln f_{BB}(ObsP^+(n) | \hat{N}_s = N_{PCR}(n), \hat{p} = \bar{P}^+(n), \hat{M} = M_{PCR}) \\ + \sum_{n,a} \ln f_{BB}(ObsS_a^+(n) | \hat{N}_s = N_{sero,a}(n), \hat{p} = \frac{S_a^+(n)}{N_a}, \hat{M} = M_{sero}). \quad \text{Equation 19}$$

Where $f_{BB}(x | \hat{N}_s, \hat{p}, \hat{M})$ is the probability function for a Beta-binomial with sample size \hat{N}_s , expected proportion of successes \hat{p} , and effective sample size \hat{M} . This was a convenient reparameterization of the Beta-binomial model under the transformation $\hat{N}_s = n, \hat{p} = \frac{\alpha}{\alpha + \beta}, \hat{M} = \alpha + \beta$ from the typical (n, α, β) parameterization. $N_{PCR}(n)$ and $N_{sero,a}(n)$ were the total number of samples (positive and negative) of, respectively, PCR test and serological tests on day n , in age group a . $\bar{P}^+(n)$ was derived from the transmission model for each day n as per above [equations 10-11]. M_{PCR} and M_{sero} were fixed from a previous modelling study.[1] The first day where samples were included in the log-likelihood calculation was 1st January 2021.

Initial conditions and model simulation. We fit to data from 1st January 2021, however, because PCR cases and serological detection are lagged indicators of infections weeks previously, we start the model simulation in each county on 1st December 2020 and use the first month of simulation to allow the simulation to converge onto the epidemic dynamics. Simulation of the model was done by solving the ODE system [equation 1] forwards from the county-specific initial conditions, with county-specific parameter configuration, using an explicit/implicit switching solver provided by the **DifferentialEquations.jl** Julia programming language package.[15]

We reduced the number of unknown parameters for the initial state of the epidemic model by considering only the overall latent infected numbers (E_0) and a scale factor on the proportion exposed

to COVID (i.e. in $R/W1/W2$ epidemiological compartments) relative to a cross-sectional survey done in Nairobi in mid-November 2020[16] which we denote τ . We fix the initial removed and waned immunity numbers as

$$\begin{aligned} R_{a,1}(0) &= N_a(0) * P_{sero,a} * \tau * 0.95, \\ W1_{a,1}(0) &= N_a(0) * P_{sero,a} * \tau * 0.05, \\ W2_{a,1}(0) &= 0. \end{aligned} \quad \text{Equation 20}$$

Where $P_{sero,a}$ was the raw (non-test sensitivity adjusted) seroprevalence estimate for Nairobi in the cross-sectional survey,[16] and τ was an adjustment factor which was added to the set of parameters to be inferred in the set θ_{TM} . Note that we are assuming that 5% of the previously exposed population have lost complete immunity to reinfection by 1st December 2020, and that no previously exposed people had completely lost immunity to reinfection. The adjustment factor τ allowed the model flexibility to represent counties with lower seroprevalence data in 2021 as having had a smaller initially exposed fraction compared to Nairobi, whilst also allowing upwards adjustment to account for the fact that the second wave of cases in Kenya occurred during the Nairobi cross-sectional study.

The age-specific numbers of initially latent infected people were derived from the next-generation matrix $K(P_{sero,1}, \dots, P_{sero,6}, \tau, \beta_0, \beta_{school}, \beta_{home}, \beta_{other}, \beta_{work})$, where we have made explicit the parameters being inferred that the next-generation matrix depends upon and its explicit dependence on the baseline seroprevalence estimates. The eigenvector \mathbf{v} , normalized such that $|\mathbf{v}|_1 = 1$, associated with the leading eigenvalue of K , represented the expected distribution of new infections across age groups. Therefore, we specified

$$\mathbf{E}(0) = E_0 \mathbf{v}. \quad \text{Equation 21}$$

Where $\mathbf{E}(0) = [E_{1,0}(0), \dots, E_{6,0}(0)]^T$. The rest of the initial variables were specified as being dependent of the flow out of the latent infected state,

$$\begin{aligned} A_{a,0}(0) &= \alpha * E_{a,0}(0) * (1 - \delta_a) / (1 + \gamma_A), \\ P_{a,0}(0) &= \alpha * A_{a,0}(0) * \delta_a / (1 + \alpha_p), \\ D_{a,0}(0) &= \alpha_p * P_{a,0}(0) * (1 - h_a) / (1 + \gamma_D). \end{aligned} \quad \text{Equation 22}$$

In every county, every individual in the model was initially unvaccinated.

Priors. In every county we used the following priors for parameter inference:

- $\epsilon \sim \text{Beta}(\hat{\alpha} = 50, \hat{\beta} = 50)$.
- $\beta_0 \sim \Gamma(\hat{k} = 10, \hat{\theta} = 1.5/10)$.
- $\beta_{other} \sim \Gamma(\hat{k} = 10, \hat{\theta} = 1.5/10)$.
- $\beta_{home} \sim \Gamma(\hat{k} = 10, \hat{\theta} = 1.5/10)$.
- $\beta_{work} \sim \Gamma(\hat{k} = 10, \hat{\theta} = 1.5/10)$.
- $\beta_{school} \sim \Gamma(\hat{k} = 10, \hat{\theta} = 1.5/10)$.
- $R_{\alpha\beta} \sim \Gamma(\hat{k} = 15, \hat{\theta} = \frac{0.4}{15})$.
- $r_{\alpha\beta} \sim \Gamma(\hat{k} = 15, \hat{\theta} = \frac{0.15}{15})$.

- $R_\delta \sim \Gamma(\hat{k} = 15, \hat{\theta} = \frac{0.6}{15})$.
- $r_\delta \sim \Gamma(\hat{k} = 15, \hat{\theta} = \frac{0.2}{15})$.
- $E_0 \sim \Gamma(\hat{k} = 3, \hat{\theta} = \frac{10000}{3})$.
- $\tau \sim \Gamma(\hat{k} = 5, \hat{\theta} = \frac{1.5}{5})$.

The prior for the PCR observation bias parameter χ , differed between counties (see below). For Nairobi and Mombasa we used a prior:

- $\chi \sim \Gamma(\hat{k} = 3, \hat{\theta} = \frac{4.5}{3})$.

MCMC draws. We used Hamiltonian MCMC with NUTS[17,18] to perform Bayesian inference by drawing 2,000 samples from the posterior distribution,

$$\theta_{TM}^{(k,c)} \sim P(\theta_{TM} | \mathcal{D}_c) \propto \exp(l(\theta_{TM}))\pi(\theta_{TM}), \text{ for } k = 1, 2, 3, \dots \quad \text{Equation 23}$$

for each county using the NUTS-HMC sampler implemented by the Julia language package *dynamicHMC.jl*. The HMC method required a log-likelihood gradient, $\nabla_\theta(l + \pi)$, which, for our use-case of an ODE system with a comparative low number of parameters (<100 parameters), was most efficiently supplied by forward-mode automatic differentiation implemented by the package *ForwardDiff.jl*. The MCMC chain converged for each county (all MCMC chains and MCMC diagnostics can be accessed through the linked open code repository.[19] The posterior mean (and 95% CIs) for each parameter can also be found in the open code repository.[19]

Approximate county-specific hierarchical model for PCR observation bias. The serological data is important for our inference because it gives information about the proportion of each age group infected at different time points, and, therefore, allows the PCR observation bias parameter (χ) to be identifiable. However, the amount of serological data differs from county to county. To allow cross-inference between counties for the bias parameter we assumed that 1) Nairobi and Mombasa were sufficiently distinct from other counties that the inferred bias parameter for these city/counties was not relevant to other counties, and 2) the other 45 counties had a bias parameter drawn from a common distribution, $\chi_c \sim \Gamma(k_\chi, \theta_\chi)$, where k_χ and θ_χ are the hyperparameters of this hierarchical model. This reflected our underlying belief that despite regional variations in transmission, the observation of data would be similar in all counties outside of the main two urban hubs.

A fully Bayesian approach to inference would involve including $\{\chi_c\}_c$ and the hyperparameters k_χ, θ_χ within a joint log-likelihood over all Kenyan counties (except Nairobi and Mombasa). However, to accelerate inference we used an approximation to this hierarchical model. The 9 counties with the most amount of serological data available, apart from Nairobi and Mombasa, were **Embu, Kilifi, Kisii, Kisumu, Kwale, Nakuru, Nyeri, Siaya, and Uasin Gishu**. We performed MCMC draws for each of these counties using a prior $\chi \sim \Gamma(\hat{k} = 3, \hat{\theta} = \frac{4.5}{3})$, which gathered a set of MCMC draws for χ from the posterior distribution for each county c , $\{\chi^{(k,c)}\}_{k=1,\dots,2000} \sim P(\chi | \mathcal{D}_c)$. We then approximated maximum a-posteriori (MAP) estimates for the hyperparameters k_χ, θ_χ using,

$$\ln P(k_\chi, \theta_\chi | \mathcal{D}_1, \dots, \mathcal{D}_9) = \ln \pi(k_\chi, \theta_\chi) + \sum_c \ln \sum_k f_\Gamma(\chi^{(k,c)} | \hat{k} = k_\chi, \hat{\theta} = \theta_\chi) + \text{const.} \quad \text{Equation 24}$$

Where f_{Γ} is the density function of a Gamma distribution, and $\ln \pi(k_{\chi}, \theta_{\chi})$ was the log-prior for the hyper-parameters. The hyper-priors used were:

- $k_{\chi} \sim \exp(\hat{\mu} = 10)$.
- $\theta_{\chi} \sim \exp(\hat{\mu} = 0.45)$.

The MAP estimation is done under the distributional assumption that the observed outcome data was distributed negative binomially with the same mean as the posterior predictive mean value (that is averaged over the posterior predictive distribution for the infection process), and a negative binomial clustering factor inferred jointly with the risk factors.

We then could use the 9 non-city counties with the most serological data to create MAP estimates \hat{k}_{χ} , $\hat{\theta}_{\chi}$ by maximizing equation 24. Equation 24 represented an approximation where we treated the MCMC draws of the χ parameter as “data” for making inference on the hyper-parameters despite using a different prior to generate the MCMC samples.

The second approximation is that for the 36 other counties that were not Nairobi, Mombasa, or one of the 9 listed above, we used a prior for χ generated from these MAP estimates

- $\chi \sim \Gamma(\hat{k} = k_{\chi}/2, \hat{\theta} = 2\theta_{\chi})$.

The reason for the scaling of 2 was to increase the prior variance for χ to reflect that we are approximating a hierarchical model.

Minimum divergence estimates for the infection outcome model

After performing MCMC we were able to estimate the posterior mean for the rate of diseased incidence, up to a proportionality with unknown risk factors $E[l_{dis,a,v,r}(n)|\mathcal{D}]$, for each day n , age group a , variant v , and county c , by solving the ODE system [equation 1] for each set of transmission model parameters drawn from the MCMC and using equation 13. We can then define the posterior expected number of deaths $\overline{Deaths}_{a,c}(n; \psi_c, \psi_r^D, \mu_a^D)$ by replacing the parameter-specific diseased incidence rate in equation 14 with its posterior mean. We define the divergence due to a choice of age dependent mortality rates (μ_a^D), relative reporting rate (ψ_c), relative variant-specific risk of death (ψ_r^D) and clustering factor α_D ,

$$Div_D(\psi_c, \psi_r^D, \mu_a^D, \alpha_D) = -2 \sum_{a,c,n} \ln f_{NB}(ObsDeaths_{a,c}(n) | \hat{\mu} = \overline{Deaths}_{a,c}(n; \psi_c, \psi_r^D, \mu_a^D), \hat{\alpha} = \alpha_D). \quad \text{Equation 25}$$

Where $f_{NB}(x|\hat{\mu}, \hat{\alpha})$ is the probability function for a negative binomial with mean $\hat{\mu}$ and clustering factor $\hat{\alpha}$, and $ObsDeaths_{a,c}(n)$ are the daily reported deaths in each age group, each county and on each day. We found a minimum point for equation 25, which we used as estimators, $\hat{\psi}_c$, $\hat{\psi}_v^D$, $\hat{\mu}_a^D$, $\hat{\alpha}_D$ (Supplementary figures 3, 4).

The ICU occupancy data was not available broken down by age or county, therefore, we assumed that the risk of reported critical disease was proportional to the risk of death for everyone and focused on fitting the relative risk of critical disease vs death μ_{rel}^{CD} . We defined the divergence between model prediction of ICU occupancy and observed occupancies due to relative risk of critical disease vs death μ_{rel}^{CD} , variant specific risk of critical disease ψ_r^C , and clustering factor α_C ,

$$Div_{ICU}(\mu_{rel}^{CD}, \psi_r^C, \alpha_C) = -2 \sum_n \ln f_{NB}(ObsICU(n) | \hat{\mu} = \sum_{a,c} \overline{ICU}_{a,c}(n; \hat{\psi}_c, \psi_r^C, \mu_{rel}^{CD}, \hat{\mu}_a^D), \hat{\alpha} = \alpha_C). \quad \text{Equation 26}$$

Where $ObsICU(n)$ was the reported Kenyan National ICU occupancy on day n , and $\overline{ICU}_{a,c}$ is the posterior mean value for the ICU occupancy with COVID. The minimum point for equation 26 gave estimators, $\hat{\psi}_v^C, \hat{\mu}_a^C = \hat{\mu}_{rel}^{CD} \hat{\mu}_a^D, \hat{\alpha}_C$ (Supplementary figures 3, 4).

The general ward occupancy data was also not available broken down by age or county, therefore, we assumed that the risk of reported severe disease was proportional to the risk of death for everyone and focused on fitting the relative risk of severe disease vs death μ_{rel}^{SD} . We defined the divergence between model prediction of general ward occupancy and observed occupancies due to relative risk of severe disease vs death μ_{rel}^{SD} , variant specific risk of severe disease ψ_r^S , and clustering factor α_S ,

$$Div_{HOSP}(\mu_{rel}^{SD}, \psi_r^S, \alpha_S) = -2 \sum_n \ln f_{NB}(ObsHOSP(n)|\hat{\mu}) = \sum_{a,c} \overline{HOSP}_{a,c}(n; \hat{\psi}_c, \psi_r^S, \mu_{rel}^{SD}, \hat{\mu}_a^D), \hat{\alpha} = \alpha_S. \quad \text{Equation 27}$$

Where $ObsHOSP(n)$ was the reported Kenyan National general ward occupancy with COVID on day n , and $\overline{HOSP}_{a,c}$ is the posterior mean value for the ICU occupancy, with the contribution from patients arriving into general wards from ICU already calculated using the minimum divergence estimates from equation 26. The minimum point for equation 27 gave estimators, $\hat{\psi}_r^S, \hat{\mu}_a^S = \hat{\mu}_{rel}^{SD} \hat{\mu}_a^D, \hat{\alpha}_S$ (Supplementary figures 3,4).

Vaccine scenario projections and immune-escape variant

Vaccination rates. We considered 7 vaccine rollout scenarios starting from 1st September 2021: No vaccination (baseline), 30%, 50%, 70% target coverage of Kenyan over 18s with either an 18 month or 6-month (rapid) time scale (Table 1). In each case we assumed that:

1. The number of vaccines deployed in each county each day was constant over the rollout.
2. Second dose followed first dose after a 56 day lag.
3. Over 50 year olds were offered the vaccine first, but demand saturated at 80% coverage among over 50 year olds (age groups 3-6 in the model) and afterwards the vaccine was offered to 18-49 year olds (age group 2).
4. Vaccines were deployed pro-rata across all disease/infection states; that is there was no dependence on past infection history in seeking vaccines.

Mathematically, this corresponds to this choice for the per-capita vaccination rate (equation 2) for the first dose, that is pro-rata distribution among all unvaccinated groups in stages by age,

$$v_{a,1}(t) = \frac{NV_{scenario}}{T_{scenario}} \frac{\mathbf{1}(\sum_{a=3,\dots,6} \sum_{v=2,\dots,5} N_{a,v} < 0.8 \sum_{a=3,\dots,6} N_a)}{\sum_{a=3,\dots,6} N_{a,1}}, \quad a = 3,4,5,6$$

$$v_{2,1}(t) = \frac{NV_{scenario}}{T_{scenario}} \frac{\mathbf{1}(\sum_{a=3,\dots,6} \sum_{v=2,\dots,5} N_{a,v} \geq 0.8 \sum_{a=3,\dots,6} N_a)}{N_{2,1}}, \quad \text{Equation 28}$$

For $1st\ sept\ 2021 \leq t \leq 1st\ sept\ 2021 + T_{scenario} - 56\ days$

Where $N_{a,v}$ is the county population by age and vaccine status (summed over disease/infection status). $\mathbf{1}(\cdot)$ is an indicator function enforcing that the vaccination rate among over 50s (age groups 3-6) drops to zero at an 80% coverage. $NV_{scenario}$ is the number of doses implied by the scenario target coverage,

and $T_{scenario}$ is the time in days over which this target coverage is to be achieved in the scenario. The second dose per capita rate is like the first dose but with doses distributed among people who have had their first dose,

$$v_{a,2}(t) = \frac{NV_{scenario}}{T_{scenario}} \frac{\mathbf{1}(\sum_{a=3,\dots,6} \sum_{v=3,\dots,5} N_{a,v} < 0.8 \sum_{a=3,\dots,6} N_a)}{\sum_{a=3,\dots,6} N_{a,2}}, \quad a = 3,4,5,6$$

$$v_{2,1}(t) = \frac{NV_{scenario}}{T_{scenario}} \frac{\mathbf{1}(\sum_{a=3,\dots,6} \sum_{v=3,\dots,5} N_{a,v} \geq 0.8 \sum_{a=3,\dots,6} N_a)}{N_{2,2}}, \quad \text{Equation 29}$$

For $1st\ sept\ 2021 + 56\ days \leq t \leq 1st\ sept\ 2021 + T_{scenario}$

Uncertainty propagation in vaccination scenarios. In this study we use a mixture of full Bayesian inference, for transmission model parameters, that were specific to each Kenyan county, and minimum divergence estimators, for outcome model parameters, that were specific to Kenyan counties, e.g. the county-specific reporting/disease rate relative to Nairobi ψ_c , or were specific to particular age groups, e.g. the baseline risk of death per infection in each age group μ_a^D .

When generating scenario projections for all Kenya, we solved the transmission model (equation 1) for each of the 47 Kenyan counties and for each of the 2000 MCMC draws of county-specific transmission model parameters. To match the 2000 MCMC draws for transmission parameters per county we drew 2000 replicates of the vaccine effectiveness from reported ranges first and second dose AstraZeneca effectiveness against Delta variant. This generated 2000 expected daily reported death incidence, ICU occupancy and general ward occupancy for each county (equations 14-15, 17) for each county) and for each of the 7 vaccine rollout scenarios.

To account for (1) uncertainty in transmission parameters, (2) unpredictability in reporting, and (3) uncertainty in vaccine effectiveness, the prediction intervals for Kenya as a total were calculated by

1. Augmenting the 2000 projections of expected daily reported observables per day, per age group, and per county into a single group of 2000 projections of expected daily reported observables per day, and per age group by summing across counties.
2. Converting from *expected* daily reported observables to *random* instances by sampling from the negative binomial distribution that minimized divergence between actual observed data and the model projections (equations 25-27) for each day of the 2000 projections.
3. Presenting the daily ensemble average (and 95% ensemble prediction intervals) across the 2000 randomized projections.

Modelling immune escape variant. In this paper we consider an immune escape variant which reduces protection against reinfection by 50% across natural immunity and vaccine protection, and spreads faster through the population with a 30% reduced generation time but is otherwise epidemiologically like the Delta variant. Concretely, we implemented this by assuming that the immune escape variant arrived in Kenya on 15th November 2021, during a period of low infections for other variants, and applying a set of instantaneous effects:

- Relative immune escape variant frequency becomes 100% in all Kenyan counties, reflecting rapid dominance of invading variant.
- All transmission rate parameters (e.g. β_0 , α , α_P , γ_D , γ_A) increase by a factor 1/0.7.

- 50% of people in fully or partially immune (post-natural infection) categories (**R**, **W1**) transition instantly to completely waned immunity to reinfection (**W2**).
- Vaccine effectiveness against reinfection and reduction of infectiousness ($\pi_2^{sus}, \pi_3^{sus}, \pi_2^{inf}, \pi_3^{inf}$) decrease by 50%.

Economic Evaluation Equations

Productivity losses

Productivity losses was calculated using the following equation:

$$PL = PL_{morbidity} + PL_{mortality}$$

Equation a

Where: PL=productivity losses; PL_{morbidity}=productivity loss due to morbidity; PL_{mortality}=productivity loss due to mortality

$$PL_{morbidity} = PL_{asymptomatic} + PL_{mild} + PL_{severe} + PL_{critical}$$

$$PL_{asymptomatic} = \text{Number of asymptomatic cases} \times \text{testing rate} \times \text{GDP per capita} \\ \times \text{quarantine period} \times \text{informal sector proportion}$$

$$PL_{mild} = \text{Number of mild cases} \times \text{testing rate} \times \text{GDP per capita} \times \text{quarantine period} \\ \times \text{informal sector proportion}$$

$$PL_{severe} = \text{Number of severe cases} \times \text{GDP per capita} \times \text{quarantine period}$$

$$PL_{critical} = \text{Number of critical cases} \times \text{GDP per capita} \times \text{duration of critical disease}$$

The testing rate was used to apportion the number of asymptomatic and mild cases who are tested. Further the proportion of informal sector is used to apply lost productivity on asymptomatic/mild cases that are in the informal sector, given the assumption that only those in informal sector are likely not to be productive as they isolate. Lastly, the duration of disease is used where the duration of illness is more than the 14 day quarantine period.

$$PL_{mortality} = YLL \times \text{GDP per capita}$$

Where: YLL=Years of life lost (described below)

Disability adjusted life years (DALYs)

Disability adjusted life years (DALYs) was calculated using the equation:

$$DALYs = \sum_a^j YLL_a + \sum_h^k YLD_h$$

Equation b

Where: *a* is the age at death; *j*= number of age groups; *h* are the health states; *k* =number of health states.

YLL is estimated as [20]:

$$YLL = \frac{KCe^{ra}}{(r + \beta)^2} \{ e^{-(r+\beta)(L+a)} [-(r + \beta)(L + a) - 1] - e^{-(r+\beta)a} [-(r + \beta)a - 1] \} + \frac{1 - K}{r} (1 - e^{-rL})$$

Equation c

Where: K=age weighting modulating factor; C=adjustment constant for age weights; r=discount rate; a=age of death; β =parameter from the age weighting function; L=standard life expectancy at age of death

Years lost due to disability (YLD) is estimated as [20]:

$$YLDs = D \left\{ \frac{KCe^{ra}}{(r + \beta)^2} \left\{ e^{-(r+\beta)(L+a)} [-(r + \beta)(L + a) - 1] - e^{-(r+\beta)a} [-(r + \beta)a - 1] \right\} + \frac{1 - K}{r} (1 - e^{-rL}) \right\}$$

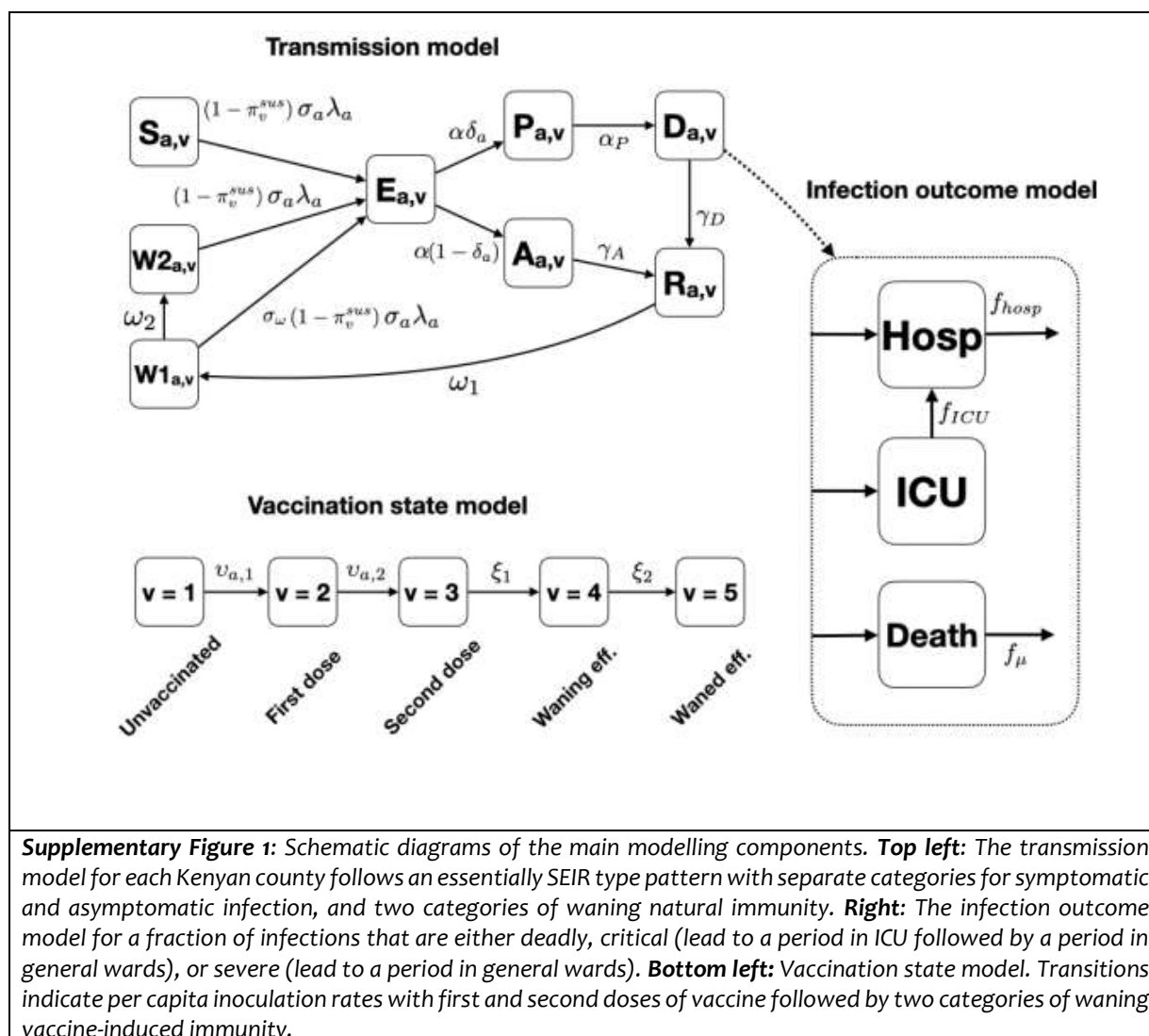
Equation (d)

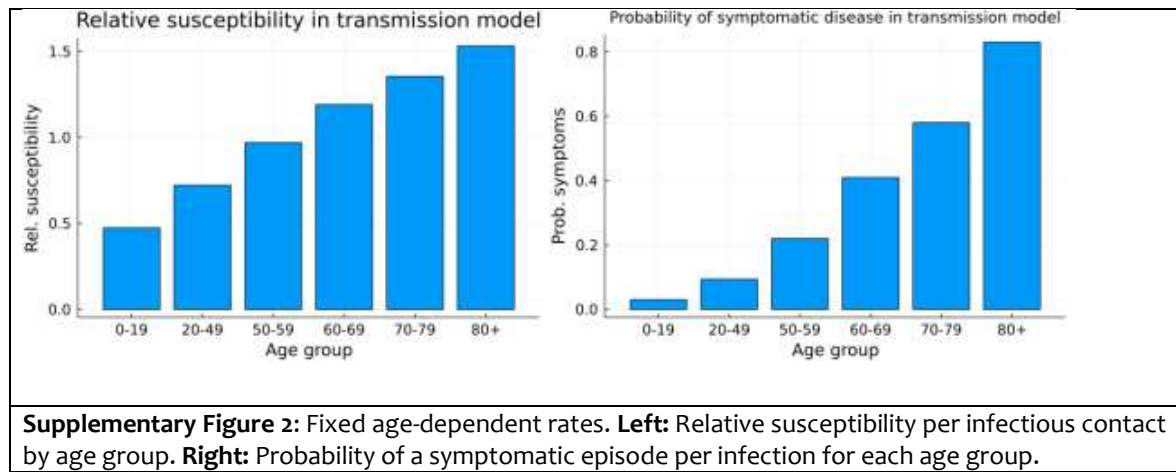
Where: K=age weighting modulating factor; C=adjustment constant for age weights; r=discount rate; a=age of onset of disability; β =parameter from the age weighting function; L=duration of disability; D=disability weight

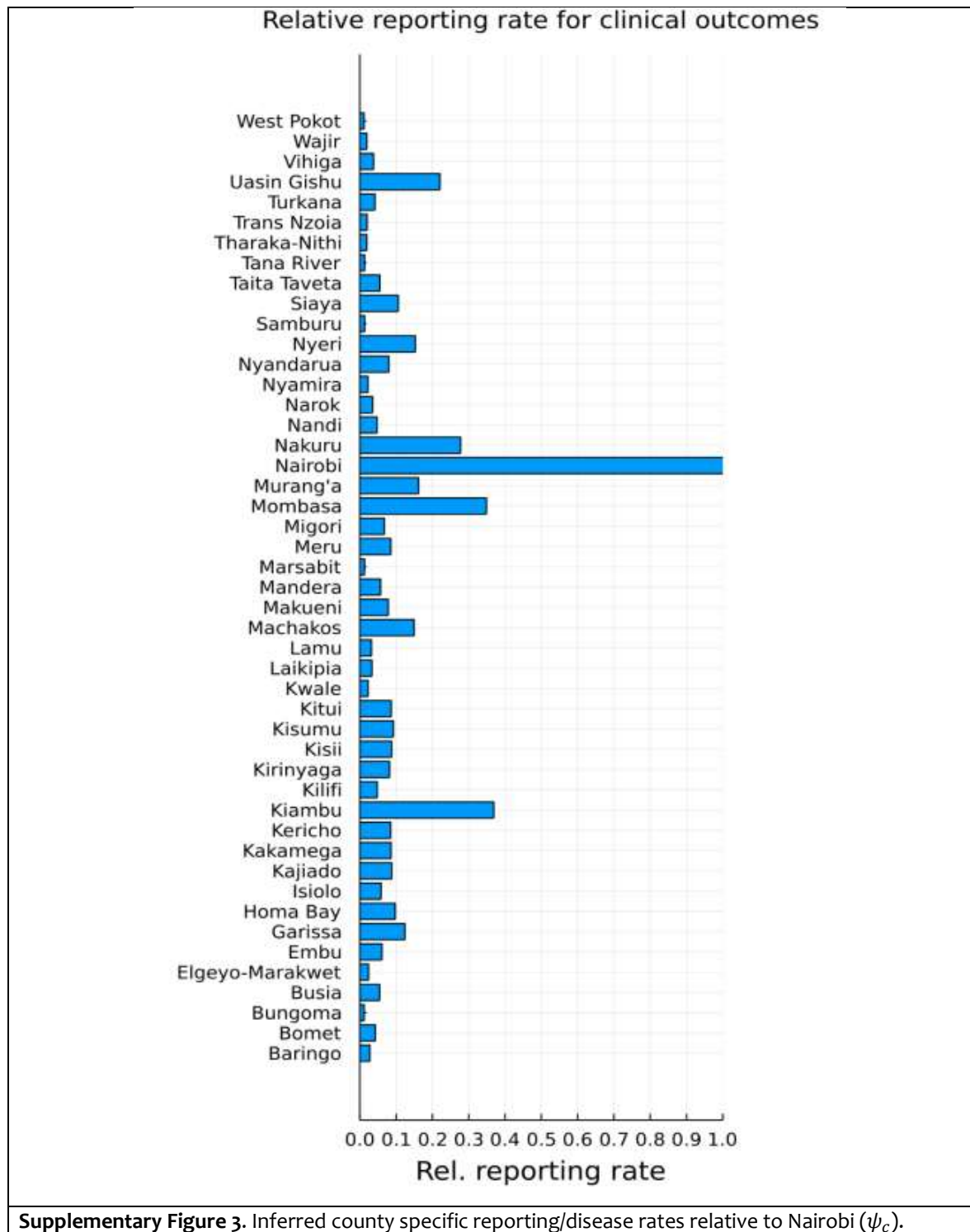
REFERENCES

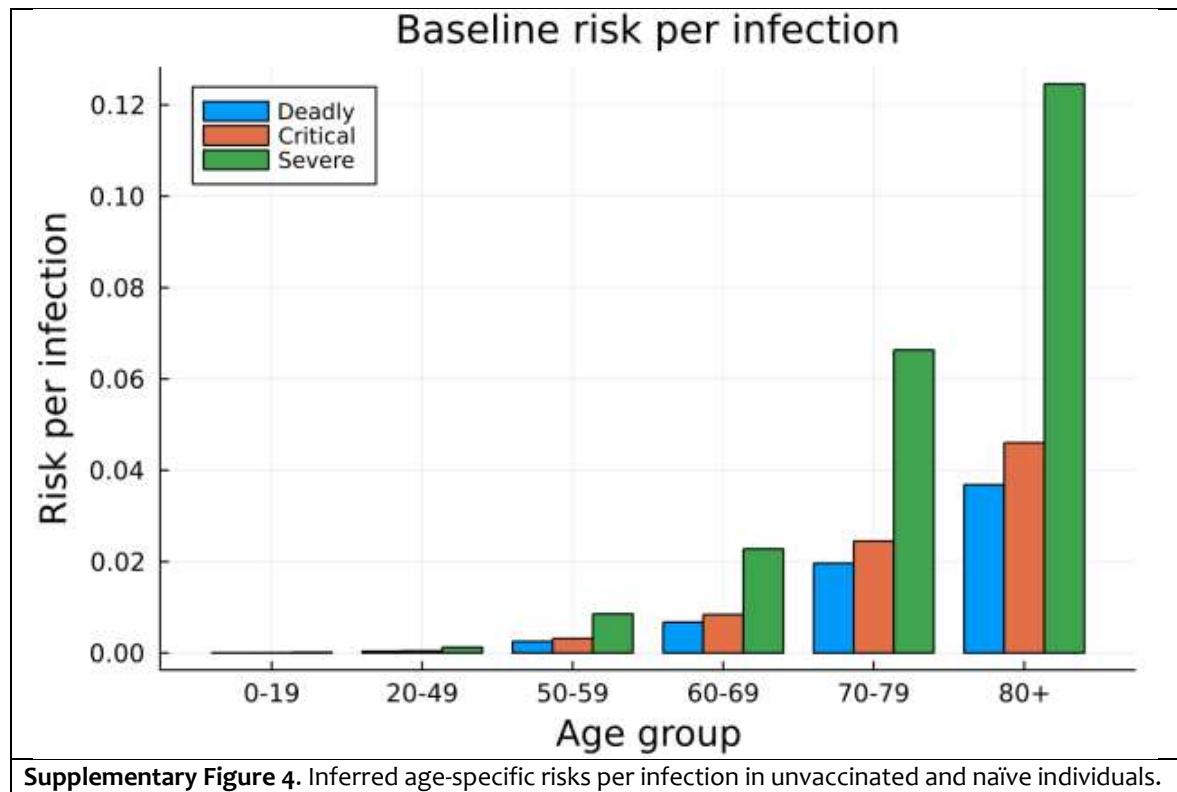
- 1 Brand SPC, Ojal J, Aziza R, et al. COVID-19 transmission dynamics underlying epidemic waves in Kenya. *Science* (80-) Published Online First: 7 October 2021. doi:10.1126/science.abk0414
 - 2 Prem K, van Zandvoort K, Klepac P, et al. Projecting contact matrices in 177 geographical regions: An update and comparison with empirical data for the COVID-19 era. *PLOS Comput Biol* 2021;17:e1009098. doi:10.1371/JOURNAL.PCBI.1009098
 - 3 Moore S, Hill EM, Dyson L, et al. Modelling optimal vaccination strategy for SARS-CoV-2 in the UK. *PLOS Comput Biol* 2021;17:e1008849. doi:10.1371/JOURNAL.PCBI.1008849
 - 4 Keeling MJ, Thomas A, Hill EM, et al. Waning, Boosting and a Path to Endemicity for SARS-CoV-2. *medRxiv* Published Online First: 10 November 2021. doi:10.1101/2021.11.05.21265977
 - 5 Google L.L.C. COVID-19 Community Mobility Reports. 2022. <https://www.google.com/covid19/mobility/> (accessed 4 Mar 2022).
 - 6 Freunde von GISAID e.V. GISAID-Tracking of Variants. 2022. <https://www.gisaid.org/hcov19-variants/> (accessed 4 Mar 2022).
 - 7 Githinji G, de Laurent ZR, Mohammed KS, et al. Tracking the introduction and spread of SARS-CoV-2 in coastal Kenya. *Nat Commun* 2021 121 2021;12:1–10. doi:10.1038/s41467-021-25137-x
 - 8 Lauer SA, Grantz KH, Bi Q, et al. The Incubation Period of Coronavirus Disease 2019 (COVID-19) From Publicly Reported Confirmed Cases: Estimation and Application. *Ann Intern Med* 2020;172:577–82. doi:10.7326/M20-0504
 - 9 Moghadas SM, Shoukat A, Fitzpatrick MC, et al. Projecting hospital utilization during the COVID-19 outbreaks in the United States. *Proc Natl Acad Sci U S A* 2020;117:9122–6. doi:10.1073/PNAS.2004064117/SUPPL_FILE/PNAS.2004064117.SAPP.PDF
 - 10 Tembo J, Maluzi K, Egbe F, et al. Covid-19 in Africa. *BMJ* 2021;372. doi:10.1136/BMJ.N457
 - 11 Bakilana A, Demombynes G, Gubbins P. Could COVID-19 deaths in Kenya be higher than official records? 2022. <https://blogs.worldbank.org/african/could-covid-19-deaths-kenya-be-higher-official-records> (accessed 10 Mar 2022).
 - 12 Moore S, Hill EM, Tildesley MJ, et al. Vaccination and non-pharmaceutical interventions for COVID-19: a mathematical modelling study. *Lancet Infect Dis* 2021;21:793–802. doi:10.1016/S1473-3099(21)00143-2/ATTACHMENT/6721682C-734C-4335-A43B-6F5B618390E1/MMC1.PDF
 - 13 Keeling MJ, Hill EM, Gorsich EE, et al. Predictions of COVID-19 dynamics in the UK: Short-term forecasting and analysis of potential exit strategies. *PLOS Comput Biol* 2021;17:e1008619. doi:10.1371/JOURNAL.PCBI.1008619
 - 14 Van Wees J-D, Osinga S, Van Der Kuip M, et al. Forecasting hospitalization and ICU rates of the COVID-19 outbreak: an efficient SEIR model. *World Heal Organ Bull* Published Online First: 2020. doi:10.2471/BLT.20.251561
 - 15 Rackauckas C, Nie Q. DifferentialEquations.jl – A Performant and Feature-Rich Ecosystem for Solving Differential Equations in Julia. *J Open Res Softw* 2017;5:15. doi:10.5334/JORS.151
 - 16 Ngere I, Dawa J, Hunsperger E, et al. High seroprevalence of SARS-CoV-2 but low infection fatality ratio eight months after introduction in Nairobi, Kenya. *Int J Infect Dis* 2021;112:25–34. doi:10.1016/j.ijid.2021.08.062
 - 17 Neal RM. MCMC Using Hamiltonian Dynamics. In: *Handbook of Markov Chain Monte Carlo*. CRC Press 2011.
 - 18 Hoffman MD, Gelman A. The No-U-Turn Sampler: Adaptively Setting Path Lengths in Hamiltonian Monte Carlo. *J Mach Learn Res* 2014;15:1351–81. <http://mcmc-jags.sourceforge.net> (accessed 10 Mar 2022).
- [dataset]19 Orangi S, Ojal J, Brand SP., et al. Data from: Epidemiological impact and cost-

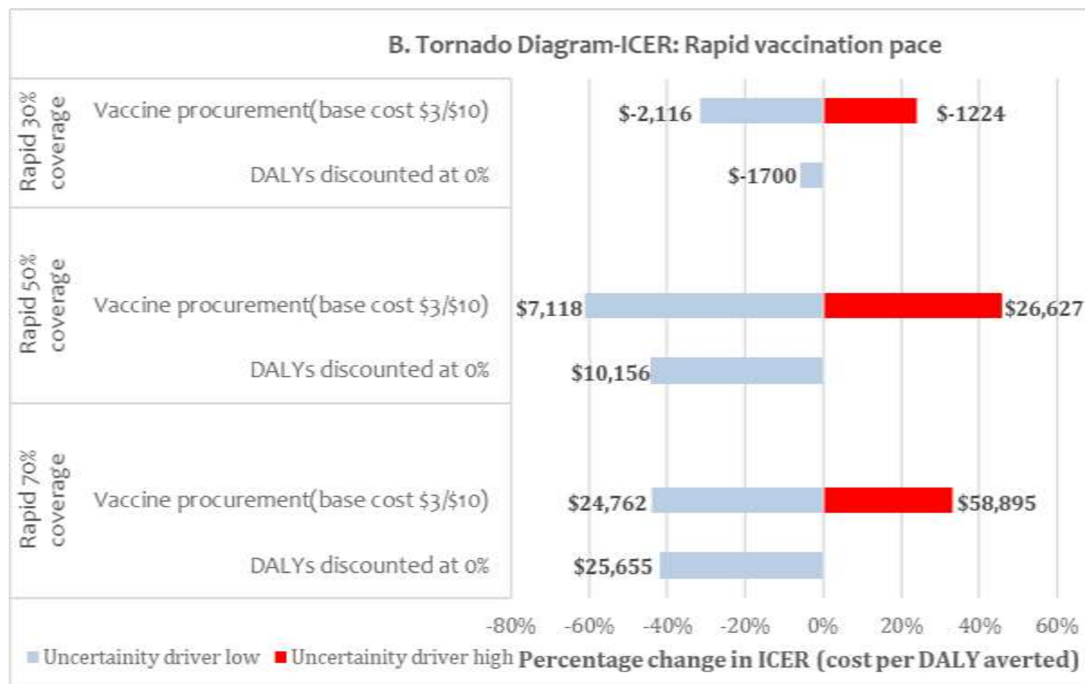
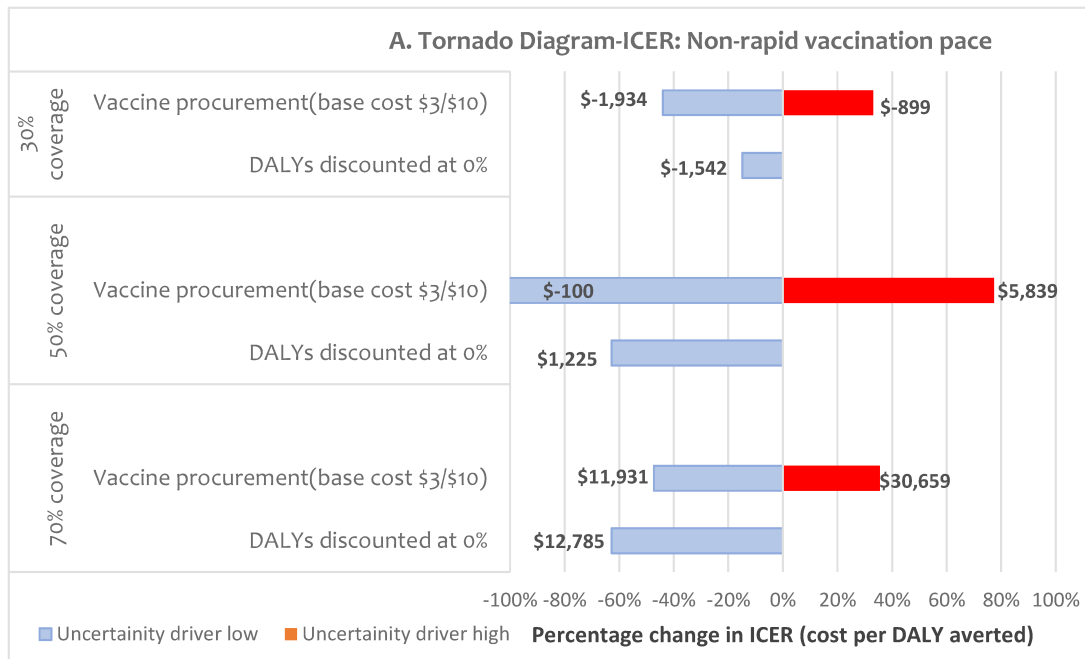
- effectiveness analysis of COVID-19 vaccination in Kenya. GitHub Repos. 2022.<https://github.com/SamuelBrand1/KenyaCoVaccines> (accessed 2 Jun 2022).
- 20 Fox-Rushby JA, Hanson K. Calculating and presenting disability adjusted life years (DALYs) in cost-effectiveness analysis. *Health Policy Plan* 2001;**16**:326–31. doi:10.1093/HEAPOL/16.3.326











Supplementary Figure 5: One-way sensitivity analysis of vaccine prices and discounting rate on ICERs

Supplementary Table 1: Transmission model parameters

Transmission model parameters and variables	Value
State Variables	
Number of susceptible people at time t, S(t)	Dynamic
Number of latently infected people at time t, E(t)	Dynamic
Number of infectious people at time t, I(t)	Dynamic
Number of recovered and immune people at time t, R(t)	Dynamic
Number of people who have lost natural immunity at time t, W(t)	Dynamic
Cumulative number of primary infections at time t, (F(t)	Dynamic
Cumulative number of all infections at time t, C(t)	Dynamic
Transmission model parameters	
Number of latently infected people at time t=0, 1 st January 2021, by age group, $E_a(0)$, $a = 1,2, \dots,6$	Inferred from data.
Background transmission, β_0	Inferred from data
Scaling from social to effective contacts at home, β_{home} , school, β_{school} , work, β_{work} and other places, β_{other}	Inferred from data
Maximum increase in transmission due to the introduction of the alpha and beta variants, $L_{\alpha\beta}$, or the delta variant, L_{δ}	Inferred from data
Growth rate of the alpha and beta variants, $\kappa_{\alpha\beta}$, or the delta variant, κ_{δ}	Inferred from data
Midpoint of the sigmoid growth curve for alpha and beta variants, $t_{0\alpha\beta}$, or the delta variant, $t_{0\delta}$	Inferred from data
A factor that translates the initial (1 st Jan -10 th Mar 2021) seroprevalence by age group to initial attack rates, τ	Inferred from data
Infectious period, $1/\gamma$	2.4 days. Chosen to recreate a serial interval of 5.5days [1]
Latent period, $1/\sigma$	3.1 days. The mean incubation period [2] was reduced by two days of pre-symptomatic transmission [3] to give a latency period.
Mean period of complete protection after a natural infection, $1/\omega$	180 days, point estimate based on reinfection studies [4-7]
Relative susceptibility compared to naïve individuals after the loss of complete protection after the first infection, σ_{ω}	$\sigma_{\omega}=0.16$. Point estimate based on reinfection studies [4-7]
c_t – contact rate	1, Equivalent to assuming contacts are back to baseline and stable
v_i - Vaccine effectiveness against transmission (delta variant)	(0%to 35.0%)-dose 1,(0% to 69.0%)-dose 2 [8]
v_a - Vaccine effectiveness against acquisition (delta variant)	(55% to 65%)-dose 1,(65% to 80%)-dose 2[9]

v_d - Vaccine effectiveness against severe disease (delta variant)	(80% to 90%) dose 1, (95% to 99%) -dose 2 [9]
v_μ - Vaccine effectiveness against death (delta variant)	(90%-95%) -dose 1, (95% to 99%) -dose 2 [9]
$1/r_{vp_i}$ - rate of vaccine progression to full efficacy	14 days after each dose ($i = 1,2$) [10]
Observation model parameters and data	
Number of people, by age group, who would test PCR positive on day n , $(P^+)_n$.	Dynamic
Number of people, by age group, who were observed to test PCR positive on day n , $(P_{obs}^+)_n$.	Data
Number of people, by age group, who would test as sero-converted on day n , $(S^+)_n$.	Dynamic
Number of people, by age group, who actually test as sero-converted on day n , $(S_{obs}^+)_n$.	Data
Probability that an infected individual would test PCR positive on day t after infection, $Q_{PCR}(t)$	$Q_{PCR}(t) = f_{onset} Q_\Gamma(\tau)$ where $Q_\Gamma(\tau)$ was the tail function of a gamma distribution fitted to data given in [11] and is the probability function of onset of symptoms post-infection [2].
Probability that an infected individual would be detectably seropositive on day t after infection, $Q_{sero}(t)$	$Q_{sero}(t)$ is linearly increasing over 26 days to saturate at 92.7% sensitivity, based on report delay in seroconversion [11] and maximum sensitivity of serological assay [12].
Relative bias in favour of selecting a PCR positive individual for testing, χ	Inferred from data
Clinical outcome parameters	
The age-dependent probability of death given severe infection, μ_a^D	Inferred from data
The age-dependent probability of critical disease given severe infection, μ_a^C	Inferred from data
The age-dependent probability of severe disease given severe infection, μ_a^S	Inferred from data
Variant specific risk of death, ψ_a^D	Inferred from data
Variant specific risk of critical disease, ψ_a^C	Inferred from data
Variant specific risk of severe disease, ψ_a^S	Inferred from data

References

- 1 Ferretti L, Wymant C, Kendall M, *et al.* Quantifying SARS-CoV-2 transmission suggests epidemic control with digital contact tracing. *Science (80-)* 2020;**368**. doi:10.1126/science.abb6936
- 2 Lauer SA, Grantz KH, Bi Q, *et al.* The Incubation Period of Coronavirus Disease 2019 (COVID-19) From Publicly Reported Confirmed Cases: Estimation and Application. *Ann Intern Med* 2020;**172**:577–82. doi:10.7326/M20-0504
- 3 Tindale LC, Stockdale JE, Coombe M, *et al.* Evidence for transmission of COVID-19 prior to symptom onset. *Elife* 2020;**9**:1–34. doi:10.7554/ELIFE.57149
- 4 Harvey RA, Rassen JA, Kabelac CA, *et al.* Association of SARS-CoV-2 Seropositive Antibody Test With Risk of Future Infection. *JAMA Intern Med* 2021;**181**:672–9. doi:10.1001/jamainternmed.2021.0366
- 5 Hall VJ, Foulkes S, Charlett A, *et al.* SARS-CoV-2 infection rates of antibody-positive compared with antibody-negative health-care workers in England: a large, multicentre, prospective cohort study (SIREN). *Lancet* 2021;**397**:1459–69. doi:10.1016/S0140-6736(21)00675-9
- 6 Vitale J, Mumoli N, Clerici P, *et al.* Assessment of SARS-CoV-2 Reinfection 1 Year After Primary Infection in a Population in Lombardy, Italy. *JAMA Intern Med* 2021;**181**:1407–8. doi:10.1001/jamainternmed.2021.2959
- 7 Lumley SF, Wei J, O'Donnell D, *et al.* The Duration, Dynamics, and Determinants of Severe Acute Respiratory Syndrome Coronavirus 2 (SARS-CoV-2) Antibody Responses in Individual Healthcare Workers. *Clin Infect Dis* 2021;**73**:e699–709. doi:10.1093/cid/ciab004
- 8 Clifford S, Waight P, Hackman J, *et al.* Effectiveness of BNT162b2 and ChAdOx1 against SARS-CoV-2 household transmission: a prospective cohort study in England. *medRxiv* Published Online First: 25 November 2021. doi:10.1101/2021.11.24.21266401
- 9 UK Health Security Agency. COVID-19 vaccine surveillance report: Week 11. 2022. https://assets.publishing.service.gov.uk/government/uploads/system/uploads/attachment_data/file/1061532/Vaccine_surveillance_report_-_week_11.pdf (accessed 6 Apr 2022).
- 10 Ewer KJ, Barrett JR, Belij-Rammerstorfer S, *et al.* T cell and antibody responses induced by a single dose of ChAdOx1 nCoV-19 (AZD1222) vaccine in a phase 1/2 clinical trial. *Nat Med* 2020;**27**:270–8. doi:10.1038/s41591-020-01194-5
- 11 Lisboa Bastos M, Tavaziva G, Abidi SK, *et al.* Diagnostic accuracy of serological tests for covid-19: systematic review and meta-analysis. *BMJ* 2020;**370**:2516. doi:10.1136/bmj.m2516
- 12 Uyoga S, Adetifa IMO, Karanja HK, *et al.* Seroprevalence of anti-SARS-CoV-2 IgG antibodies in Kenyan blood donors. *Science (80-)* 2021;**371**:79–82. doi:10.1126/science.abe1916

Supplementary Table 2: Statistical distributions for the probabilistic sensitivity analysis

	Statistical distribution*
Costs	
Vaccine delivery cost per patient at 30% coverage	Gamma (10055,6.1E-4)
Vaccine delivery cost per patient at 50% coverage	Gamma (13679,3E-4)
Vaccine delivery cost per patient at 70% coverage	Gamma (9221,4E-4)
Unit treatment cost of an asymptomatic patient	Gamma (103.1,9.6E-4)
Unit treatment cost of a mild case	Gamma (105.1,1.8E-1)
Unit treatment cost of a severe case	Gamma (105.1,1.2)
Unit treatment cost of a critical case	Gamma (105.1,5.7)
Health outcomes	
Disability weight for a critical case	Beta (102.8,54.2)
Disability weight for a severe case	Beta (21.6,140.8)
Disability weight for a mild case	Beta (21.3,396.2)
Length of hospitalization for severe episode	Gamma (53.3,3.6E-4)
Length of ICU stay for critical episode	Gamma (53.3,3.6E-4)

*The form of the distributions was chosen according to the nature of the parameter. (i.e. parameters describing the probability of health outcomes occurrence of an event are given by a beta distribution, while the values of the vaccine delivery costs and length of hospitalization/ICU stay of the various scenarios were described using a gamma distribution).

Supplementary Table 3: Projected costs and the cost-effectiveness of different vaccination strategies in Kenya from a health system's perspective

	Economic Outcomes				
	Total vaccine costs (\$ million) Median (2.5 th to 97.5 th percentile)	Total treatment costs (\$million) Median (2.5 th to 97.5 th percentile)	Total health care costs (\$million) Median (2.5 th to 97.5 th percentile)	Total DALYs (thousands) Median(95%CI)	ICER, USD per DALY averted Mean (95%CI)
Non-rapid vaccination pace (administered within 1.5years)					
No vaccination	-	313 (269 to 405)	313 (269 to 405)	247 (243 to 252)	-
30% coverage	236 (233 to 238)	157 (135 to 199)	393 (371 to 436)	114 (110 to 118)	555 (553 to 557)
50% coverage	323 (321 to 324)	140 (120 to 177)	463 (444 to 501)	101 (97 to 104)	5,195 (5,190 to 5,199)
70% coverage	443 (441 to 445)	133 (115 to 169)	576 (560 to 612)	96 (92 to 100)	24,535 (24,514 to 24,557)
Rapid vaccination pace (administered within 6 months)					
No vaccination	-	313 (269 to 405)	313 (269 to 405)	247 (243 to 252)	-
30% coverage	236 (233 to 238)	129 (111 to 163)	366 (347 to 399)	93 (89 to 96)	291 (290 to 295)
50% coverage	323 (321 to 324)	124 (107 to 157)	447 (430 to 481)	88 (85 to 92)	20,157 (20,126 to 20,128)
70% coverage	443 (441 to 445)	121 (104 to 152)	564 (549 to 596)	86 (82 to 89)	46,150 (46,025 to 46,274)

Costs=rounded off to the nearest 1,000,000; Total DALY rounded off to the nearest 1,000; ICERs=rounded off to the nearest whole number